

Supporting Information for:

Group 7 Carbonyl Complexes of a PNN-Heteroscorpionate Ligand

Jorge P. Valdivieso III^a, Alexander N. Erickson, and James R. Gardinier*^a

Table of Contents:

Crystal data and structure refinement tables	S2
Structures of Manganese complexes	S4
Possible Isomers of ([pz ₂ TTP]Re(CO) ₃ Br]	S5
¹ H and ³¹ P NMR of 1 in CD ₃ CN	S6
¹ H and ³¹ P NMR of 1 in CD ₂ Cl ₂	S7
PXRD of as-formed 1 before crystallization	S8
¹ H, ¹³ C, and ³¹ P NMR spectra 2-Re , 2-Mn , 3-Re , 3-Mn	S9
Thermal conversion 2-Mn to 3-Mn	S13
¹ H NMR spectrum of 2-Re at different concentrations	S14
IR spectra	S15
Electronic Absorption Spectrum of CH ₃ CN solutions of 2-Re and 3-Re	S17
Cyclic voltammograms	S17
Powder X-ray diffractogram of product after photoirradiation of 2-Mn	S18
Summary of DFT data Table	S20
Calculated IR data	S21
Calculated redox potentials	S23
Frontier orbitals	S24
Tabulated TD-DFT Data	S27
Electron density difference plots for first excited states	S32
Plot of ³¹ P NMR chemical shift versus Mulliken Charge	S32

Table S1. Crystal data and structure refinement of rhenium compounds.

Identification code	1	2-Re	3-Re
CCDC #	2371547	2371549	2371551
Empirical formula	C ₃₀ H ₂₅ N ₄ O ₃ PBrRe	C ₃₁ H ₂₅ N ₄ O ₆ F ₃ PSRe	C ₃₂ H ₂₈ F ₃ N ₅ O ₅ PReS
Formula weight	786.62	855.78	868.82
Temperature/K	100.00(10)	100.00(10)	100.00(10)
Crystal system	monoclinic	triclinic	monoclinic
Space group	P2 ₁ /n	P-1	P2 ₁ /n
a/Å	12.3314(2)	8.9587(3)	16.6364(3)
b/Å	13.5371(2)	12.2629(4)	12.9137(2)
c/Å	17.3610(3)	14.9571(5)	16.6780(3)
α/°	90	99.615(2)	90
β/°	102.9290(10)	90.746(2)	111.962(2)
γ/°	90	94.564(2)	90
Volume/Å ³	2824.62(8)	1614.38(9)	3323.04(11)
Z	4	2	4
ρ _{calc} g/cm ³	1.850	1.760	1.737
μ/mm ⁻¹	10.932	9.027	8.766
F(000)	1528.0	840.0	1712.0
Crystal size/mm ³	0.321 × 0.2 × 0.12	0.102×0.061×0.033	0.384 × 0.272 × 0.056
Cu Kα (λ)	1.54184	1.54184	1.54184
2Θ range	8.014 to 141.296	7.336 to 141.244	8.92 to 141.214
Index ranges	-14 ≤ h ≤ 15, -16 ≤ k ≤ 16, -21 ≤ l ≤ 20	-10 ≤ h ≤ 10, -14 ≤ k ≤ 14, -18 ≤ l ≤ 18	-20 ≤ h ≤ 19, -14 ≤ k ≤ 15, -19 ≤ l ≤ 20
Reflections collected	26425	29459	30852
Independent reflections	5354 [R _{int} = 0.0475, R _{sigma} = 0.0292]	6116 [R _{int} = 0.0745, R _{sigma} = 0.0478]	6303 [R _{int} = 0.0698, R _{sigma} = 0.0434]
Data/restraints/parameters	5354/0/380	6116/0/426	6303/0/436
Goodness-of-fit on F ²	1.138	1.034	1.052
Final R indexes [I>=2σ (I)]	R ₁ = 0.0302, wR ₂ = 0.0719	R ₁ = 0.0349, wR ₂ = 0.0856	R ₁ = 0.0345, wR ₂ = 0.0839
Final R indexes [all data]	R ₁ = 0.0337, wR ₂ = 0.0737	R ₁ = 0.0384, wR ₂ = 0.0881	R ₁ = 0.0431, wR ₂ = 0.0897
Largest diff. peak/hole / e Å ⁻³	0.97/-1.07	1.61/-1.29	2.00/-1.14

Table S2. Crystal data and structure refinement of manganese compounds.

Identification code	2-Mn	3-Mn_{0.92}·2-Mn_{0.08}	3-Mn_{0.84}·2-Mn_{0.16}	4
CCDC #	2371550	2383876 C _{31.92} H _{27.77} F ₃ MnN _{4.92} O _{5.08} PS	2371552 C _{31.84} H _{27.51} F ₃ MnN _{4.84} O _{5.16} PS	2371553 C ₂₈ H ₂₅ F ₃ Mn _{0.5} N ₄ O ₄ PS
Empirical formula	C ₃₁ H ₂₅ N ₄ O ₆ F ₃ PSMn			
Formula weight	724.52	736.57	735.42	629.02
Temperature/K	100.00(10)	100(2)	100.00(10)	99.9(3)
Crystal system	monoclinic	monoclinic	monoclinic	triclinic
Space group	P2 ₁ /c	P2 ₁ /n	P2 ₁ /n	P-1
a/Å	11.99461(14)	16.4795(2)	16.4795(2)	9.3815(3)
b/Å	14.01447(15)	12.8391(2)	12.8391(2)	12.9857(4)
c/Å	19.1860(2)	16.5133(3)	16.5133(3)	13.0750(5)
α/°	90	90	90	64.443(3)
β/°	96.0115(11)	111.4813(18)	111.4813(18)	85.597(3)
γ/°	90	90	90	88.991(3)
Volume/Å ³	3207.40(6)	3251.19(10)	3251.19(10)	1432.55(9)
Z	4	4	4	2
ρ _{calcg/cm³}	1.500	1.505	1.502	1.458
μ/mm ⁻¹	5.021	4.949	4.950	3.781
F(000)	1480.0	1510	1507.0	647.0
Crystal size/mm ³	0.41 × 0.201 × 0.139	0.289 × 0.145 × 0.106	0.534 × 0.295 × 0.028	0.148 × 0.095 × 0.06
Cu Kα (λ)	1.54184	1.54184	1.54184	1.54184
2Θ range	7.41 to 141.22 -14 ≤ h ≤ 14, -16 ≤ k ≤ 17, -22 ≤ l ≤ 21	6.482 to 161.666 -20 ≤ h ≤ 20, -16 ≤ k ≤ 16, -20 ≤ l ≤ 20	8.976 to 141.082 -19 ≤ h ≤ 20, -15 ≤ k ≤ 15, -19 ≤ l ≤ 20	7.516 to 141.074 -11 ≤ h ≤ 11, -15 ≤ k ≤ 15, -15 ≤ l ≤ 15
Index ranges				
Reflections collected	29938	151831	30350	26350
Independent reflections	6088 [R _{int} = 0.0356, R _{sigma} = 0.0238]	7086 [R _{int} = 0.0382]	6176 [R _{int} = 0.0397, R _{sigma} = 0.0260]	5431 [R _{int} = 0.0371, R _{sigma} = 0.0252]
Data/restraints/parameters	6088/0/427	7086 / 103 / 516	6176/0/446	5431/0/378
Goodness-of-fit on F ²	1.046	1.044	1.032	1.042
Final R indexes	R ₁ = 0.0293, wR ₂ = 0.0742	R ₁ = 0.0261, wR ₂ = 0.0693	R ₁ = 0.0347, wR ₂ = 0.0894	R ₁ = 0.0307, wR ₂ = 0.0785
[I>=2σ (I)]				
Final R indexes [all data]	R ₁ = 0.0321, wR ₂ = 0.0761	R ₁ = 0.0262, wR ₂ = 0.0694	R ₁ = 0.0383, wR ₂ = 0.0922	R ₁ = 0.0340, wR ₂ = 0.0815
Largest diff. peak/hole / e Å ⁻³	0.41/-0.30	0.317/-0.382	0.502/-0.397	0.37/-0.35

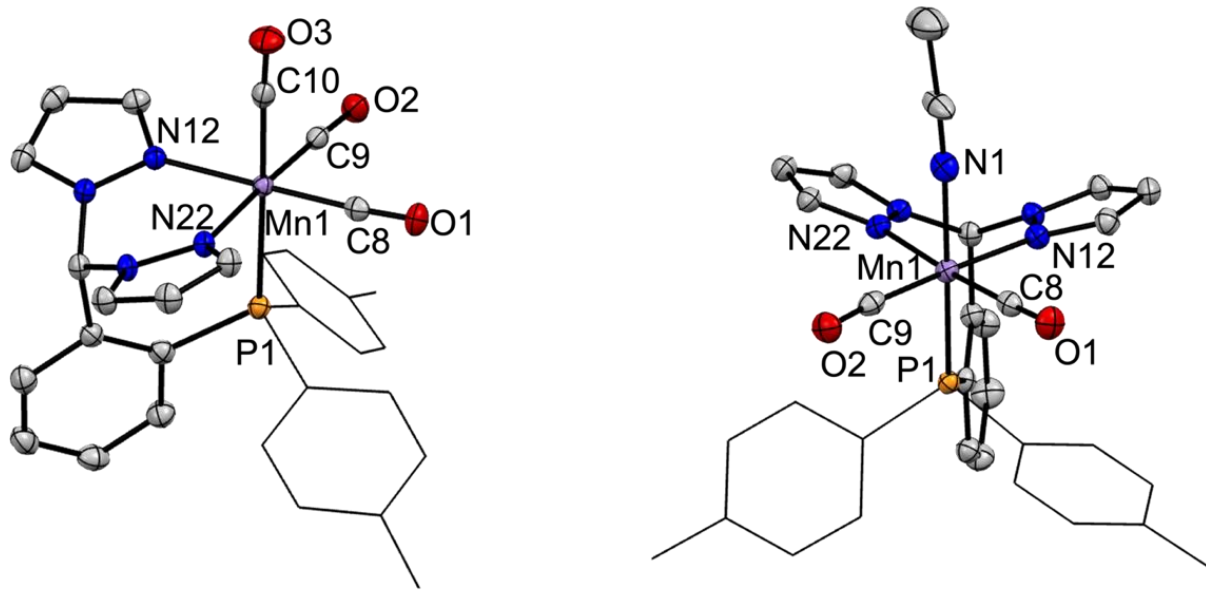


Figure S1. Structures of cations in **2-Mn** (left) and **3-Mn** (right). See Table 1 of main text for bond metrics. Thermal ellipsoids are drawn at the 50% probability level.

Possible Isomers of $[(\text{pz}_2\text{TPP})\text{Re}(\text{CO})_3\text{Br}]$, 1. There are nine reasonable isomers (excluding enantiomerism) for monomeric **1** with six-coordinate rhenium, as illustrated for a truncated model in Figure S2. There is one ionic $[\text{fac-}(\kappa^3\text{N}_2\text{P}-\text{pz}_2\text{TPP})\text{Re}(\text{CO})_3](\text{Br})$ and eight molecular

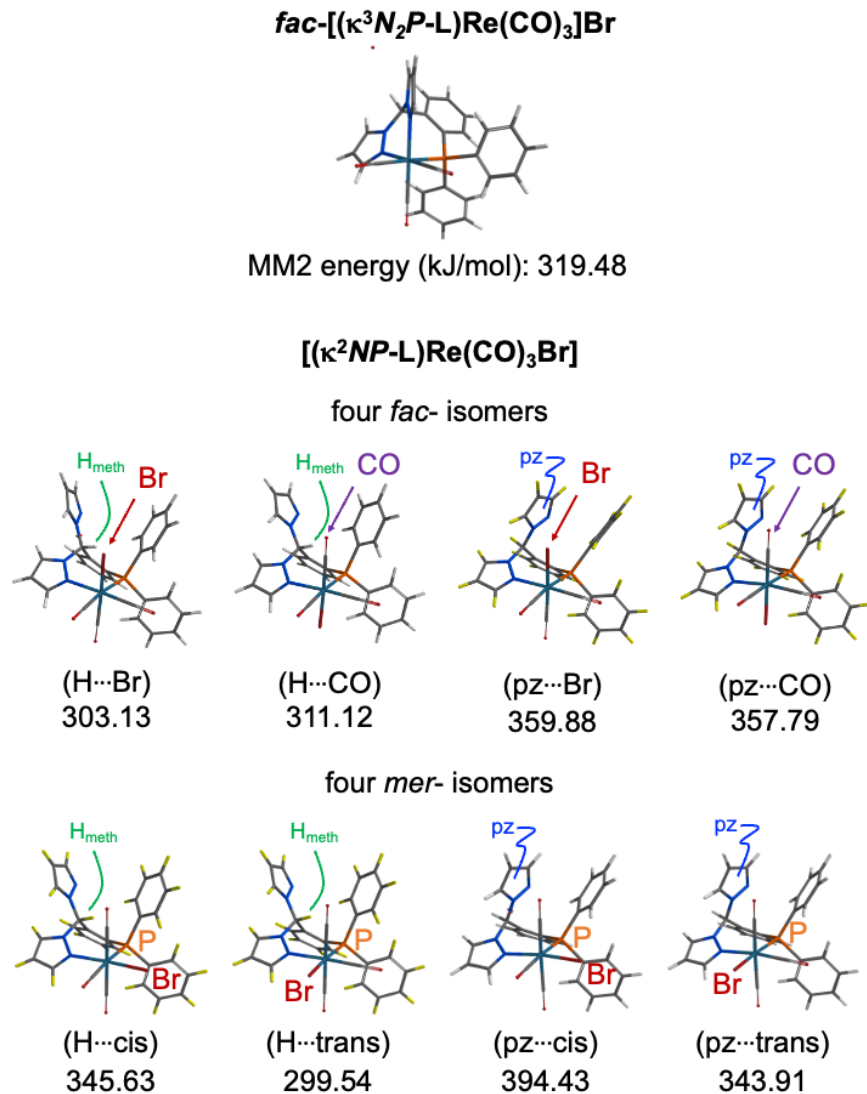


Figure S2. Possible isomers of $[(\text{pz}_2\text{TPP})\text{Re}(\text{CO})_3\text{Br}]$.

species with a $\kappa^2\text{NP}$ - ligand. Of these latter, four can have *mer*- $\text{Re}(\text{CO})_3$ moieties with the remaining being *fac*- $\text{Re}(\text{CO})_3$ derivatives. All the $\kappa^2\text{NP}$ - derivatives possess seven-membered chelate rings with the methine carbon at the bow and the Re-P bond at the stern of a boat conformation. Both the methine and Re center are chiral centers. The methine carbon can have either a hydrogen or the unbound pz pointing inside the boat. The *fac*-($\kappa^2\text{NP}$)- derivatives always have CO's *trans*- to the P- and bound pz nitrogen. So, either a Re-Br or a Re-CO can sit inside the boat. Thus, the four *fac*-($\kappa^2\text{NP}$)- isomers can be distinguished by the substituents sitting inside the boat: (H...Br), (H...CO), (pz...Br), or (pz...CO). For *mer*-($\kappa^2\text{NP}$)- isomers, a Re-CO is always inside the boat. However, the bromide can either be *cis*- or *trans*- to the phosphorous. So, four isomers are distinguished: (H...cis), (H...trans), (pz...cis), and (pz...trans). Steric

analysis using molecular models (MM2 energy) suggested the three lowest energy (κ^2NP)-isomers are (H···trans) < (H···Br) < (H···CO). Higher level DFT calculations (M06L/Def2-TZVP/PCM CH₃CN) indicate the latter two are nearly degenerate and lower energy than the former (vide infra, Table S3). However, the single crystal X-ray diffraction identified only (H···Br, major) and (H···CO, minor). NMR and PXRD studies on crude samples indicate up to four isomers might be formed in the crude reaction. After crystallization from either CH₂Cl₂/hexane or toluene/hexane, two isomers predominate. Figures S3 and S4 show the NMR spectrum of single crystals dissolved in different solvents (CD₃CN, and CD₂Cl₂, respectively). Where resonances for major isomers are labeled IA.B and minor isomers IIA,B, etc. Figure S5 shows PXRD data of crude sample before crystallization.

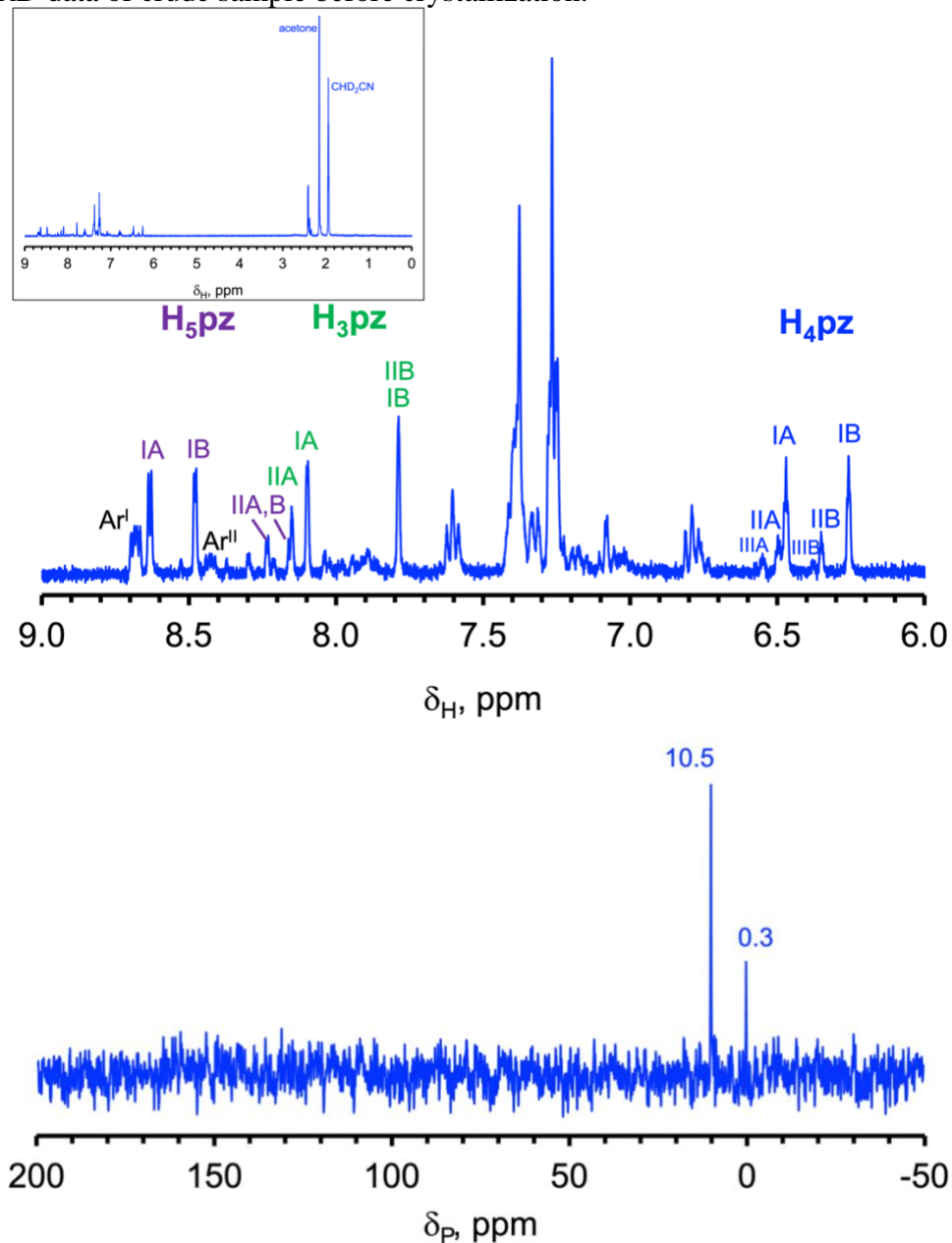


Figure S3. ¹H NMR (top with inset) and ³¹P NMR (bottom) spectra of single crystals of **1** dissolved in CD₃CN.

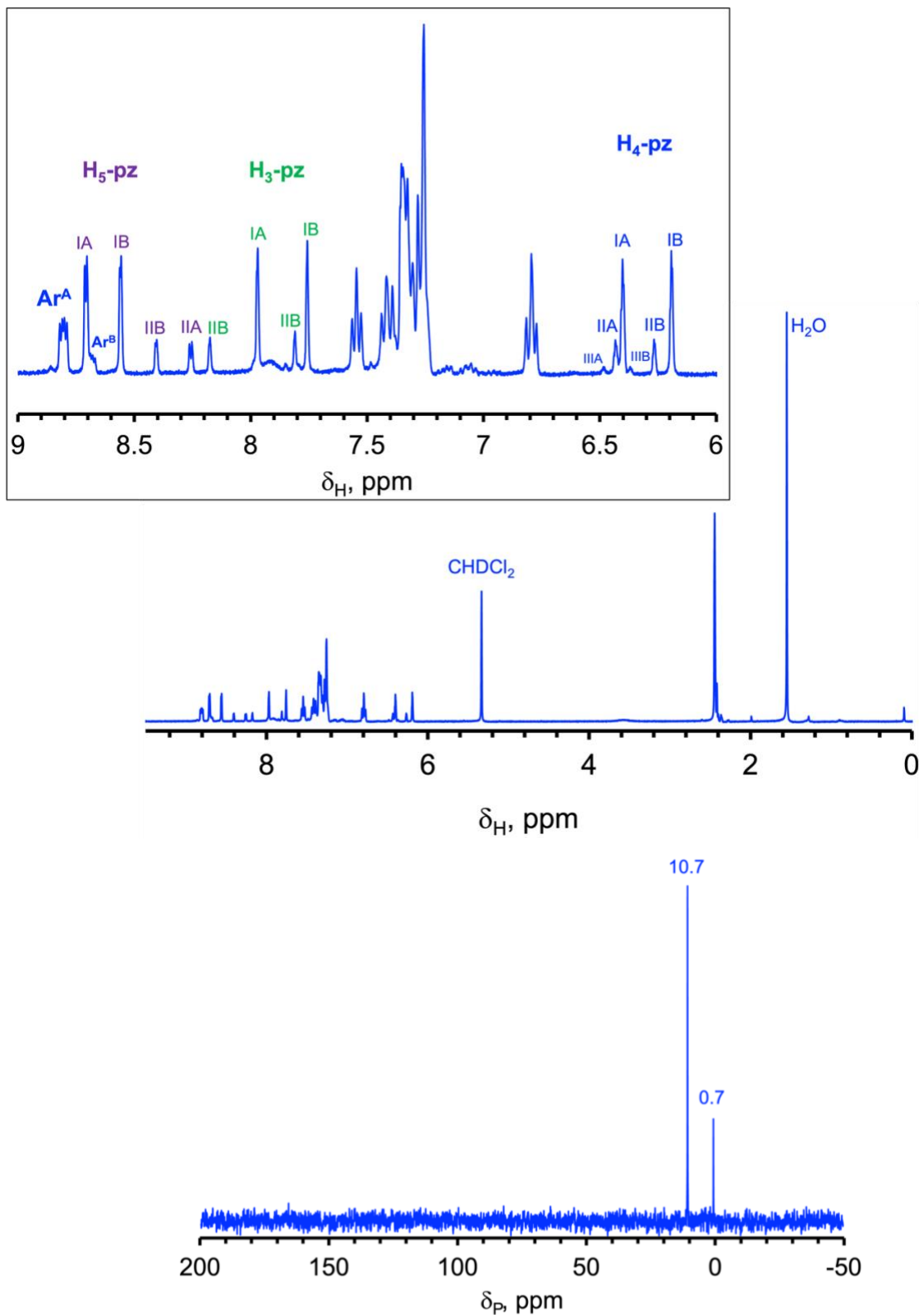


Figure S4. ${}^1\text{H}$ NMR (top with inset) and ${}^{31}\text{P}$ NMR (bottom) spectra of single crystals of **1** dissolved in CD_2Cl_2 .

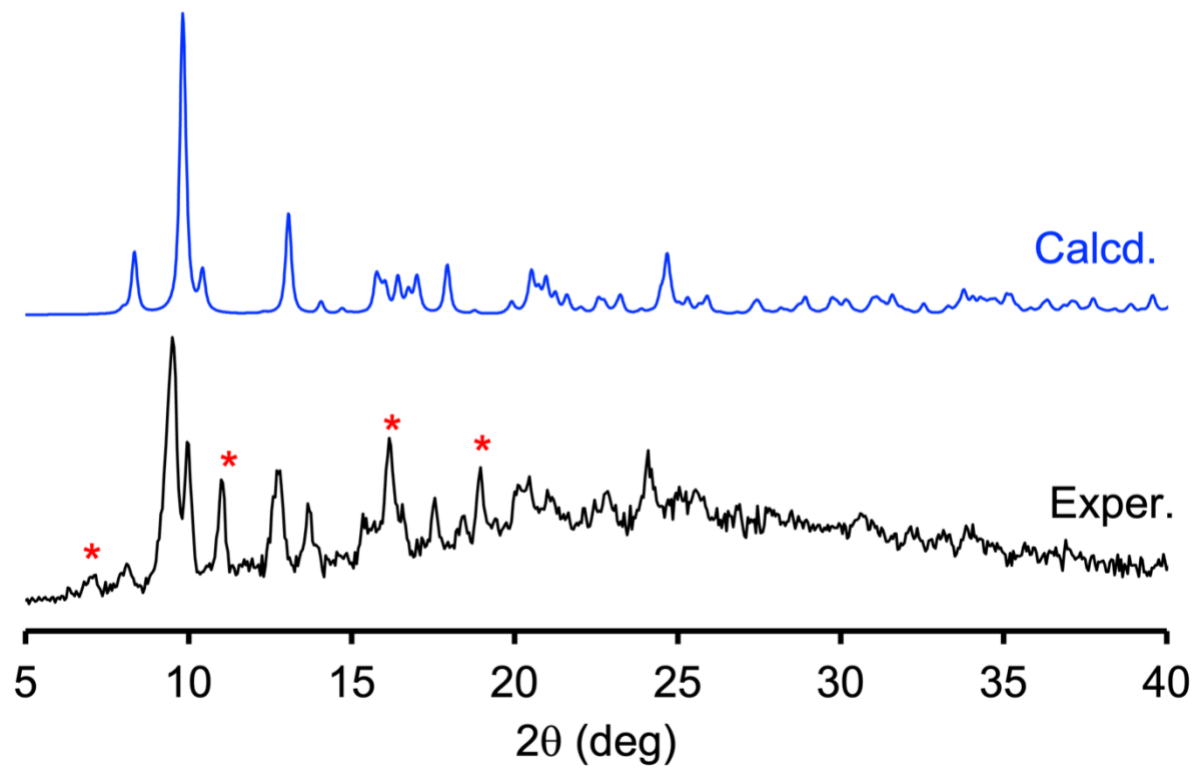


Figure S5. PXRD of powder obtained from synthesis of 1 prior to crystallization. The diffractogram labeled “Calcd”, is that calculated from single crystal diffraction data of solvate-free 1. The red asterisks in the experimental spectra are attributed to a new crystalline phase, likely fac- $[(\kappa^3N_2P\text{-}pz_2TTP)\text{Re}(\text{CO})_3](\text{Br})$.

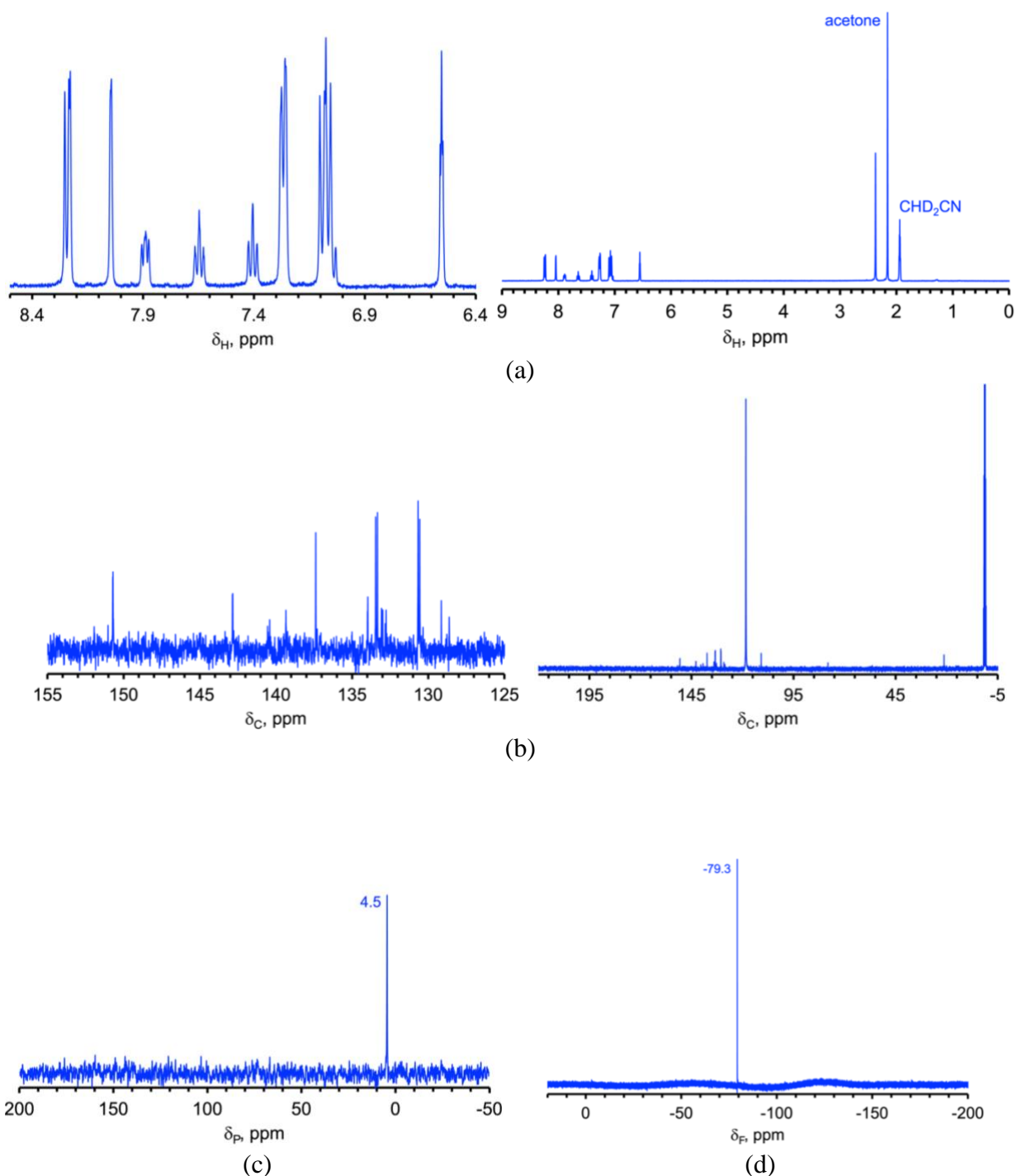
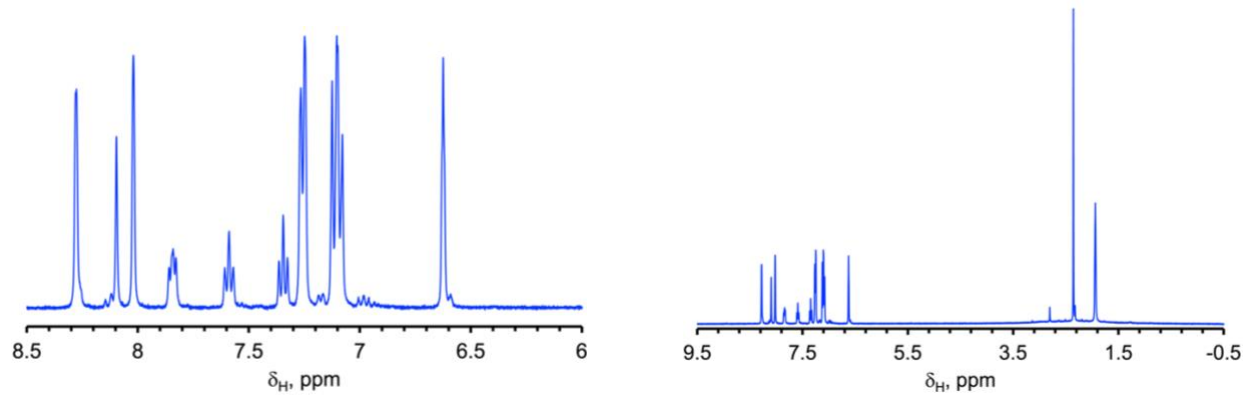
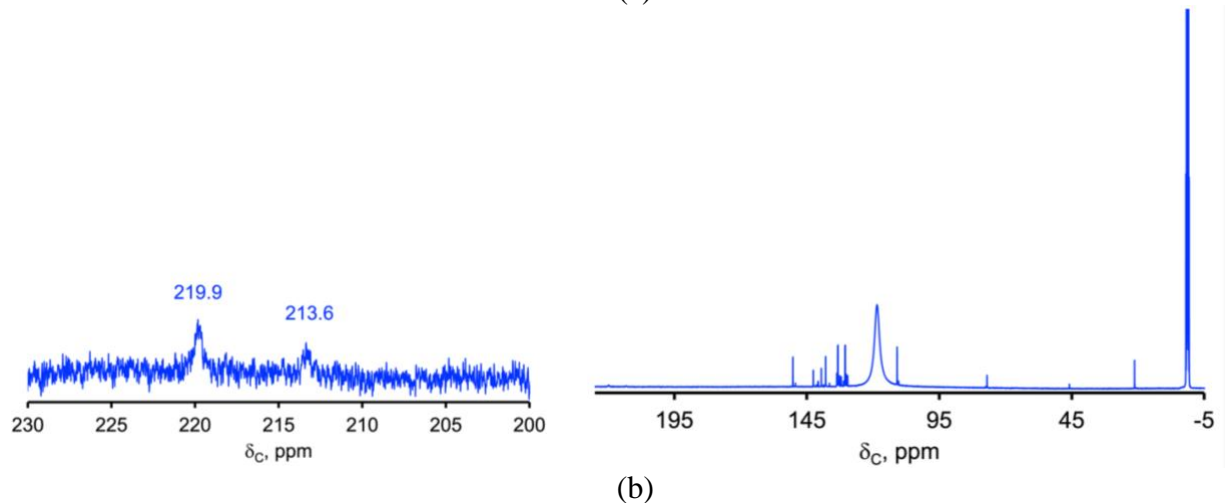


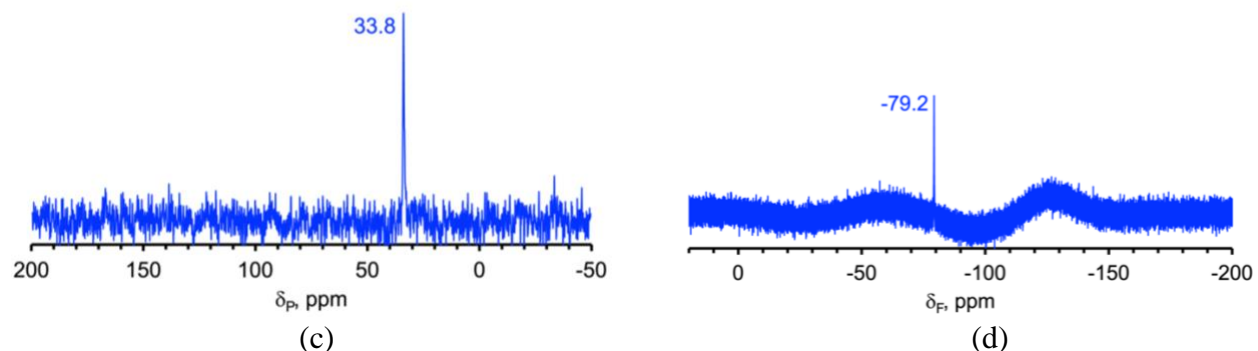
Figure S6. (a) ${}^1\text{H}$ (b) ${}^{13}\text{C}$ (c) ${}^{31}\text{P}$ and (d) ${}^{19}\text{F}$ NMR spectra of **2-Re** in CD_3CN .



(a)



(b)



(c)

(d)

Figure S7. (a) ^1H (b) ^{13}C (c) ^{31}P and (d) ^{19}F NMR spectra of **2-Mn** in CD_3CN .

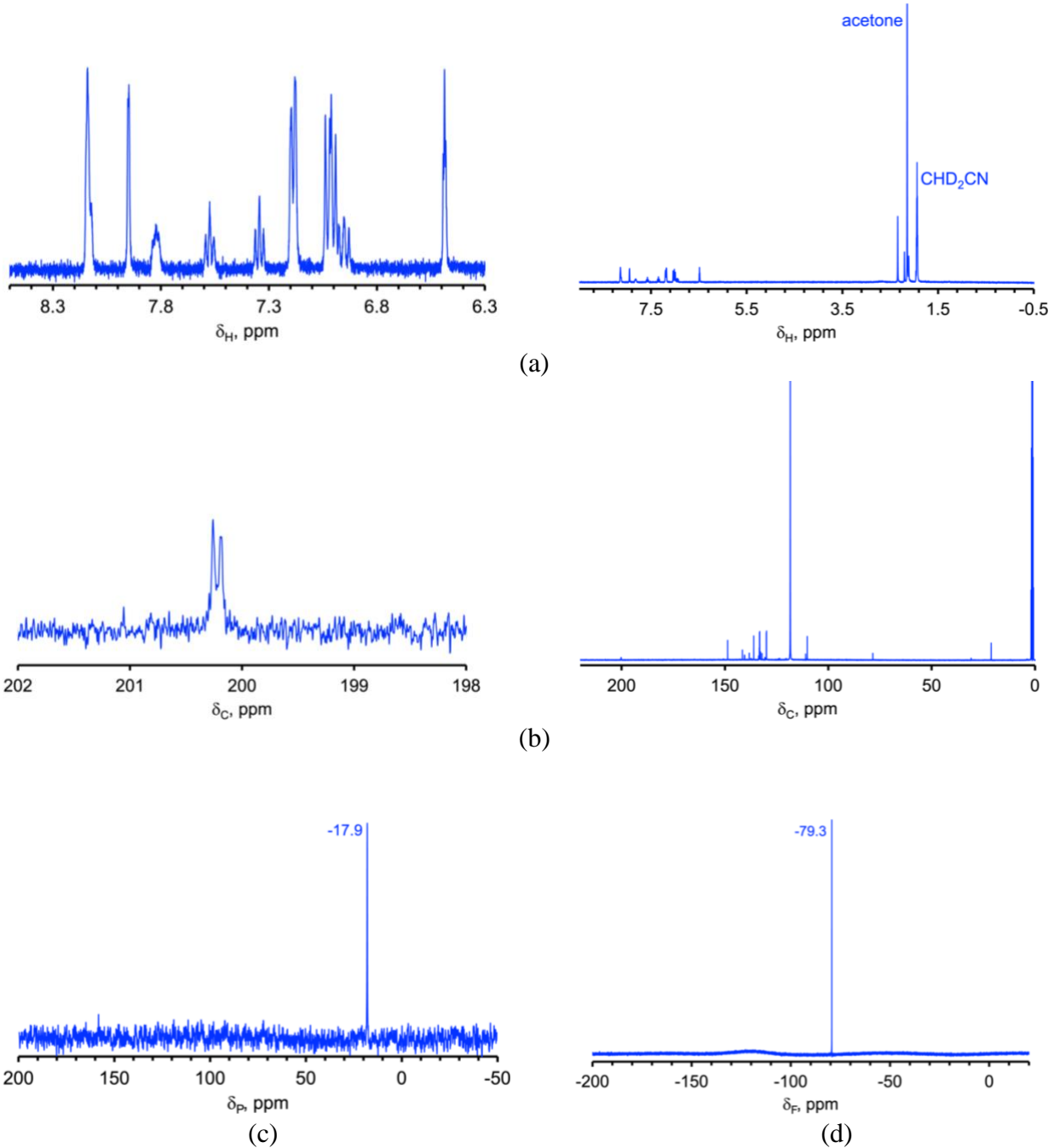
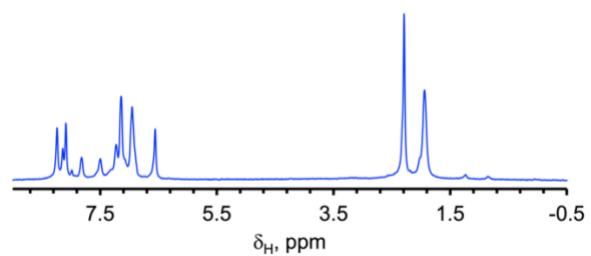
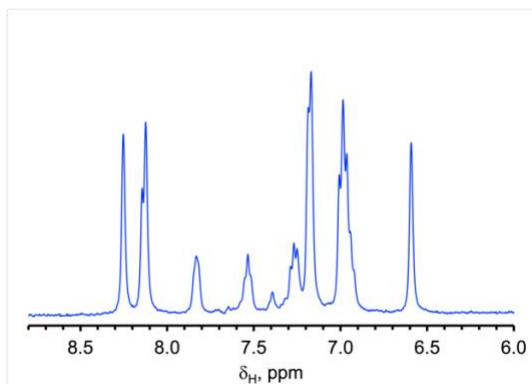
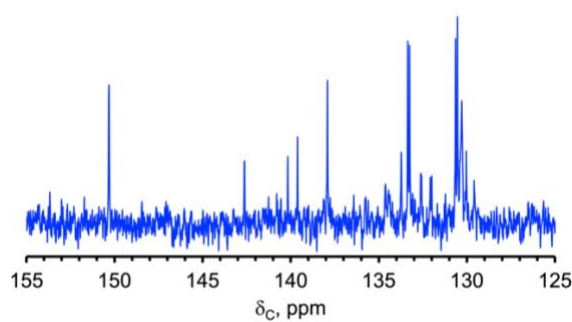


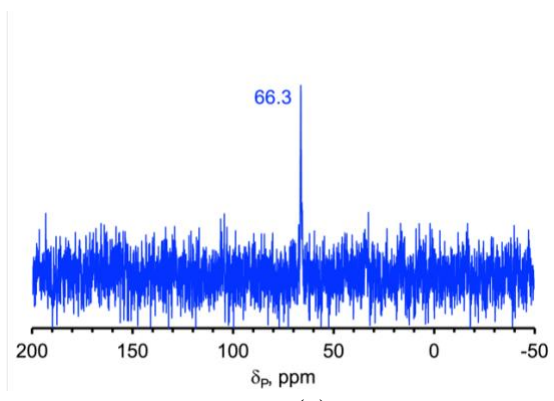
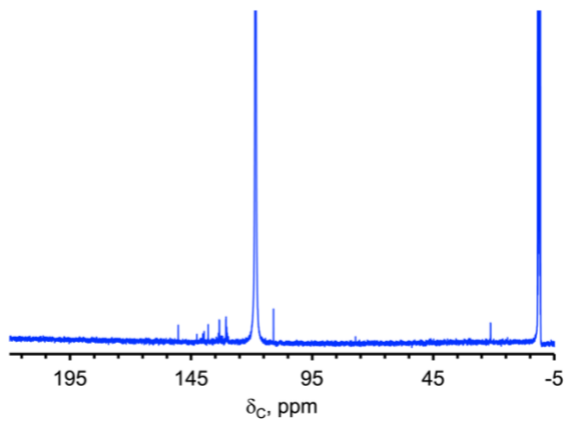
Figure S8. (a) ^1H (b) ^{13}C (c) ^{31}P and (d) ^{19}F NMR spectra of **3-Re** in CD_3CN .



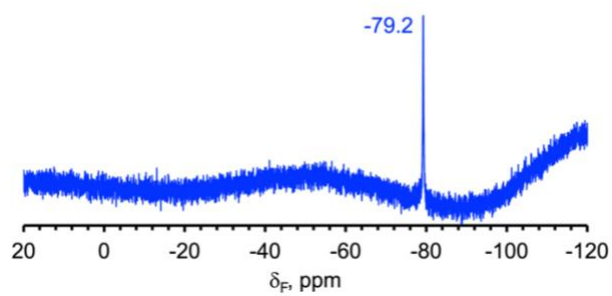
(a)



(b)



(c)



(d)

Figure S9. (a) ^1H (b) ^{13}C (c) ^{31}P and (d) ^{19}F NMR spectra of **3-Mn** in CD_3CN .

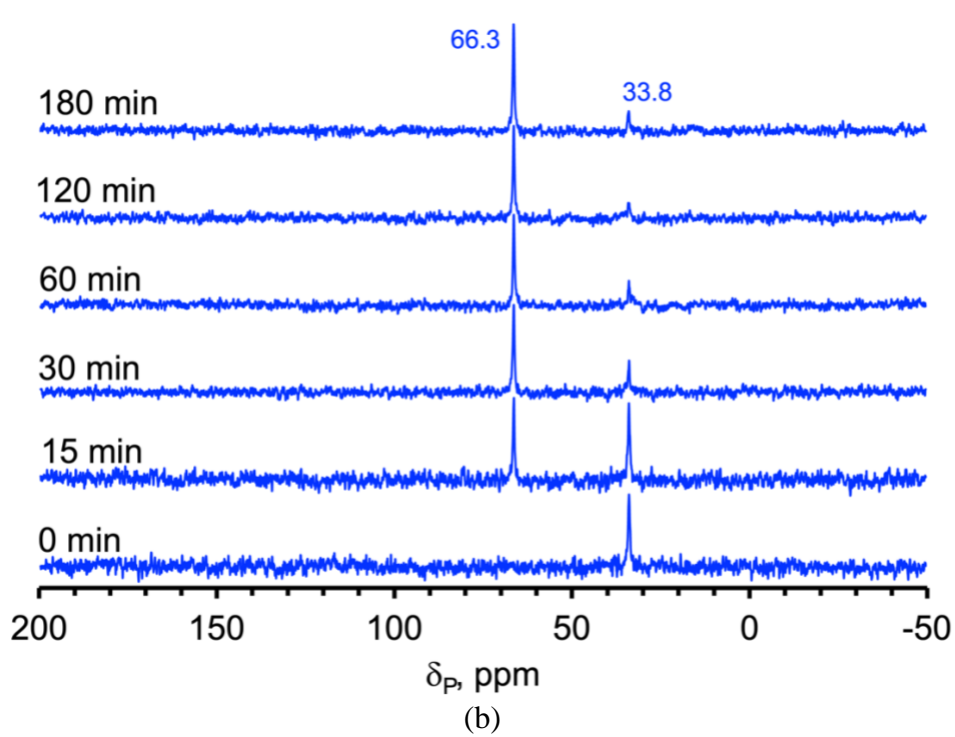
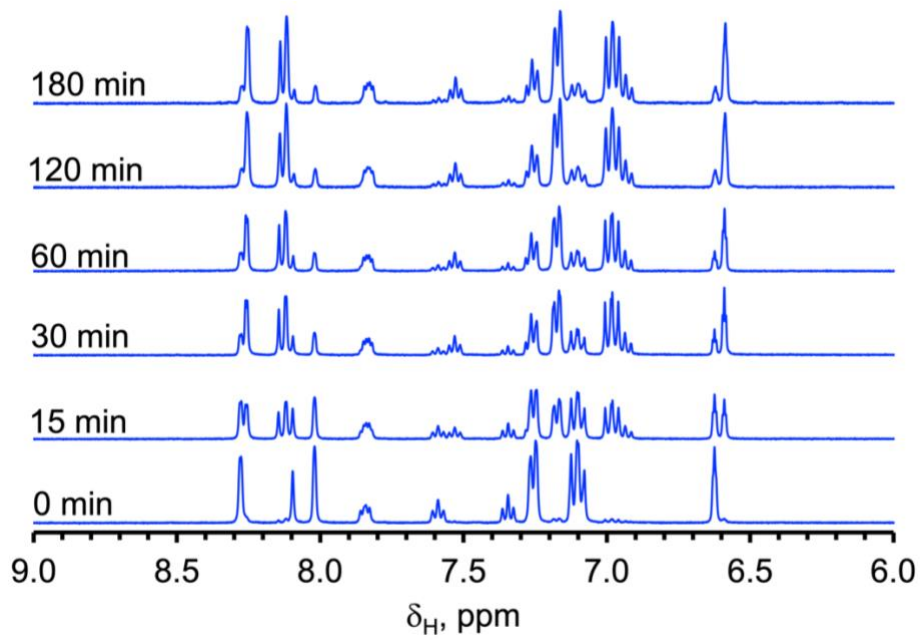
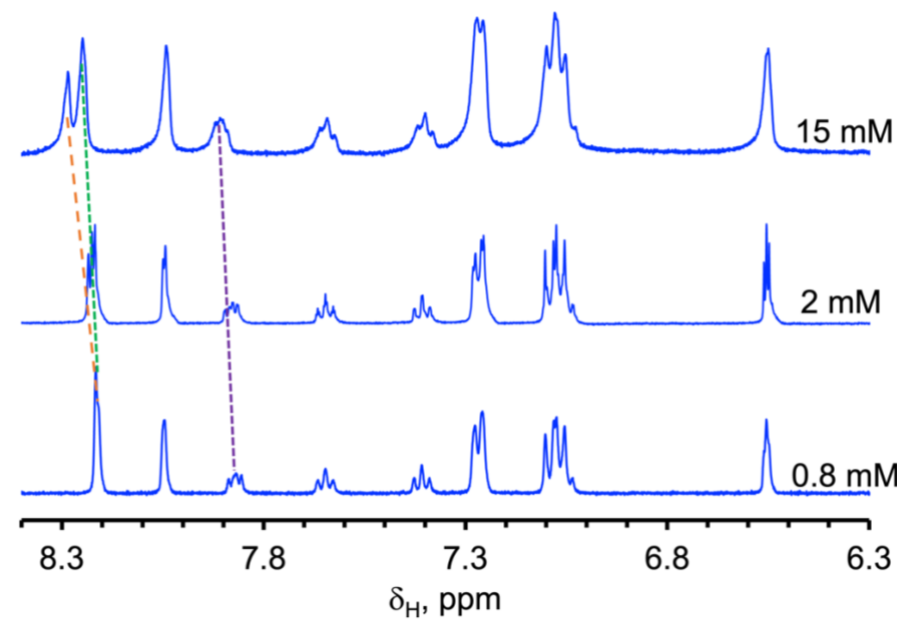
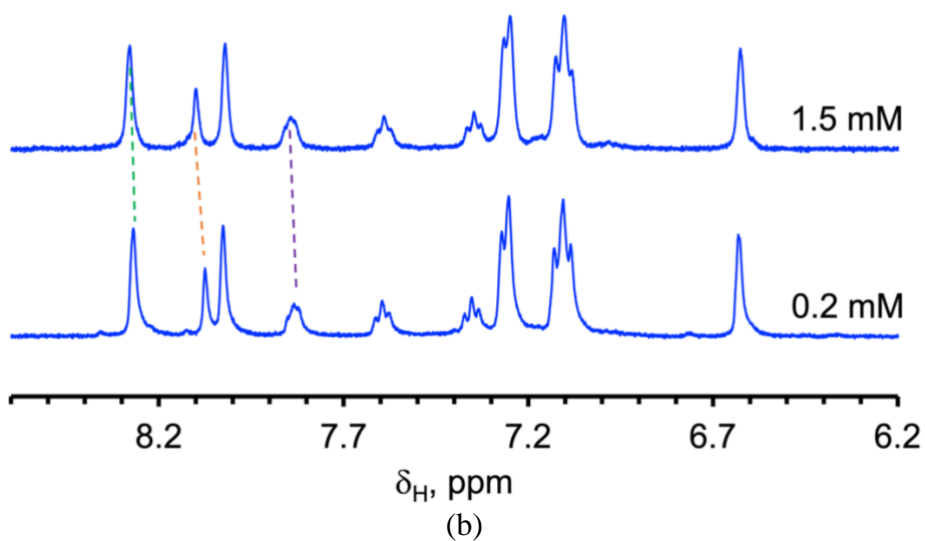


Figure S10. Overlay of ^1H (a) and ^{31}P (b) NMR spectra obtained before (bottom) and after heating a closed tube containing a CD_3CN solution of **2-Mn** in an 80°C oil bath for designated time periods.

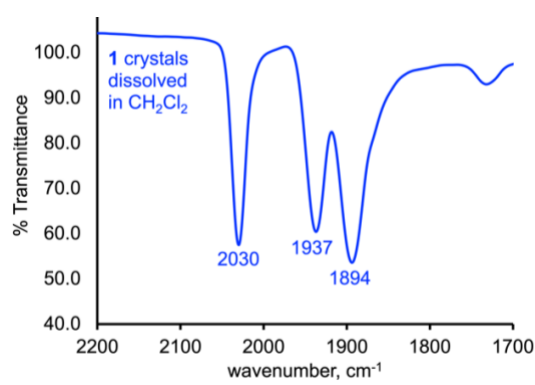
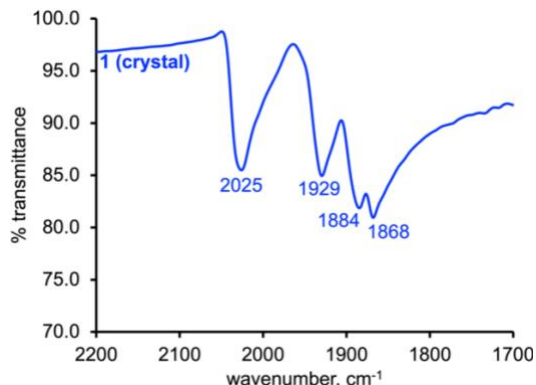


(a)

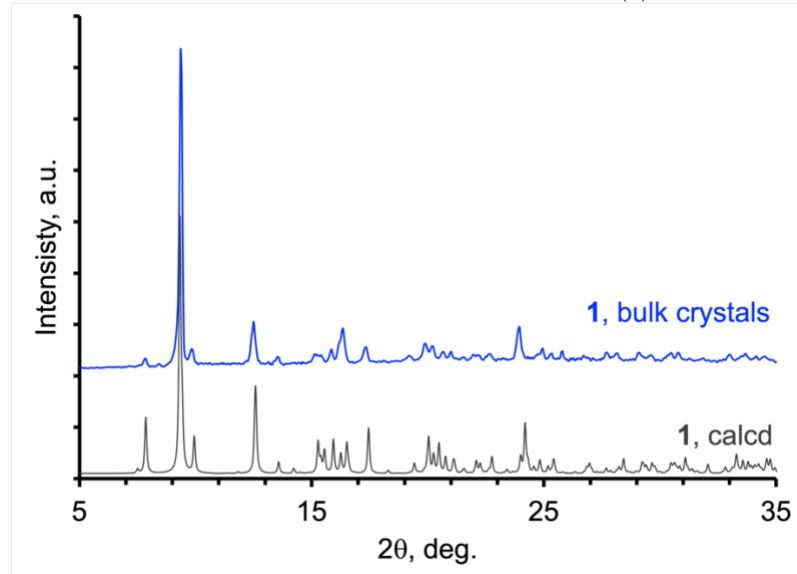


(b)

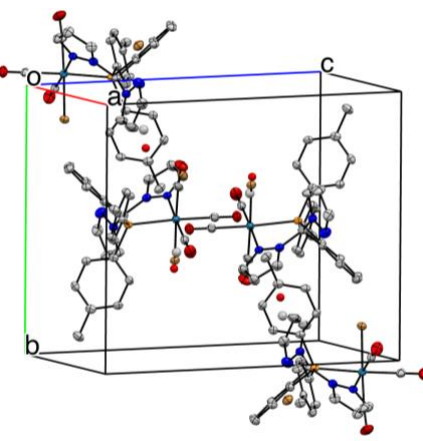
Figure S11. ¹H NMR spectra obtained for various concentrations of **2-Re** (a) or **2-Mn** (b) in CD_3CN . Dotted lines show resonances that shift frequency. Orange dashed line is for $\text{H}_{\text{methine}}$, green dashed line corresponds to H_{spz} and purple dashed line is for H_{3Ar} . The other resonances do not shift.



(a)



(b)



(c)

Figure S12. (a) Carbonyl stretching region of IR spectrum of bulk crystals of **1** in solid state and after crystals are dissolved in CH_2Cl_2 . (b) 295 K PXRD spectrum of the same sample of bulk crystals of **1** compared to that calculated from the 100 K single crystal diffraction data. (c) View of packing of unit cell.

The observation of four CO stretches in the solid spectrum of analytically pure single crystals of **1** Figure S12a (left) was clearly unexpected. Dissolving the crystals in CH_2Cl_2 gives the expected three bands Figure S12a (right). The powder diffractogram shows only one phase (Figure S12b). So, the unexpected number of bands may be due to crystal packing effects whereby the low symmetry about a dimer of molecules in the unit cell (Figure S12c) may be responsible for splitting bands.

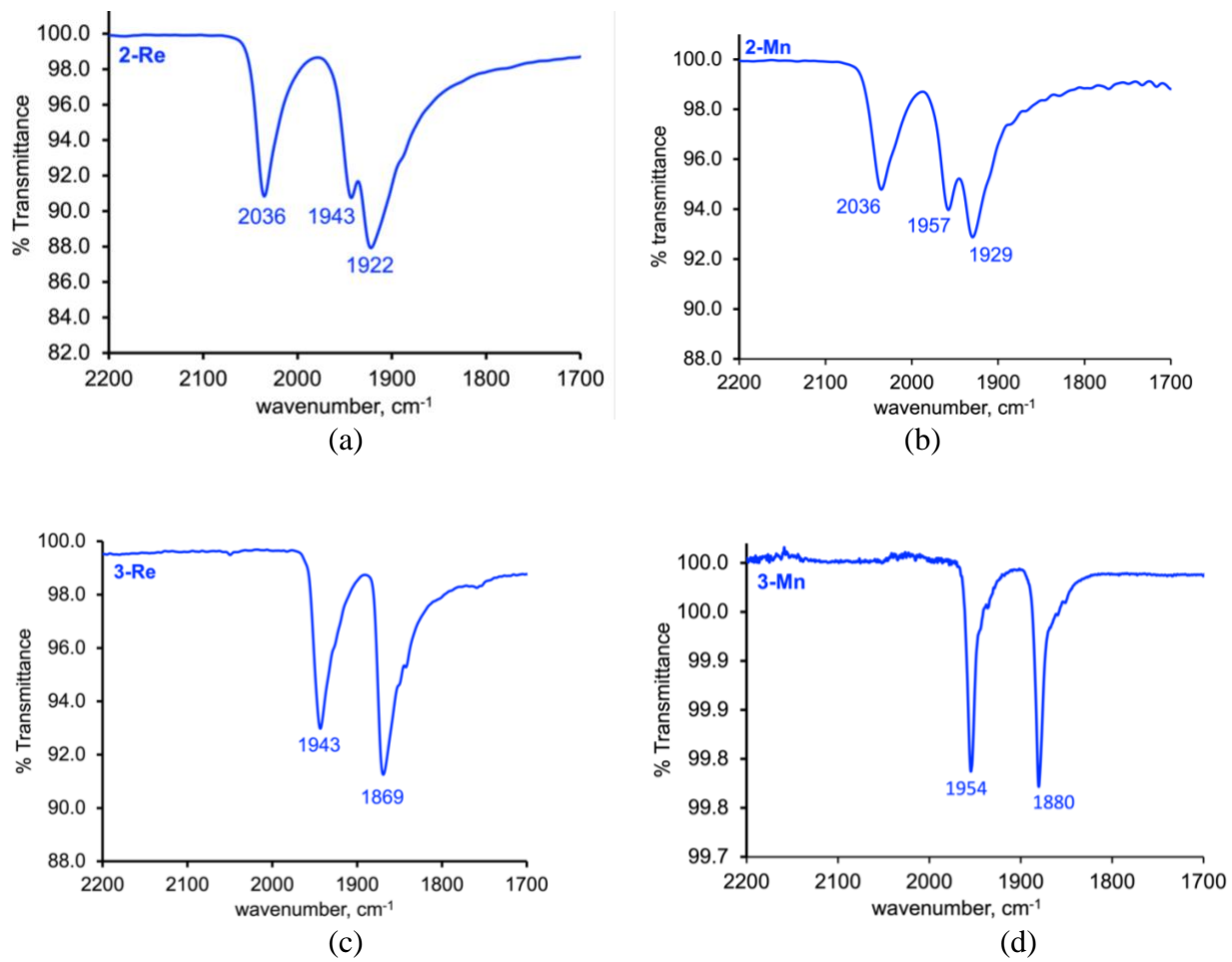


Figure S13. Carbonyl stretching region of solid-state IR spectra of (a) **2-Re**, (b) **2-Mn**, (c) **3-Re**, and (d) **3-Mn**.

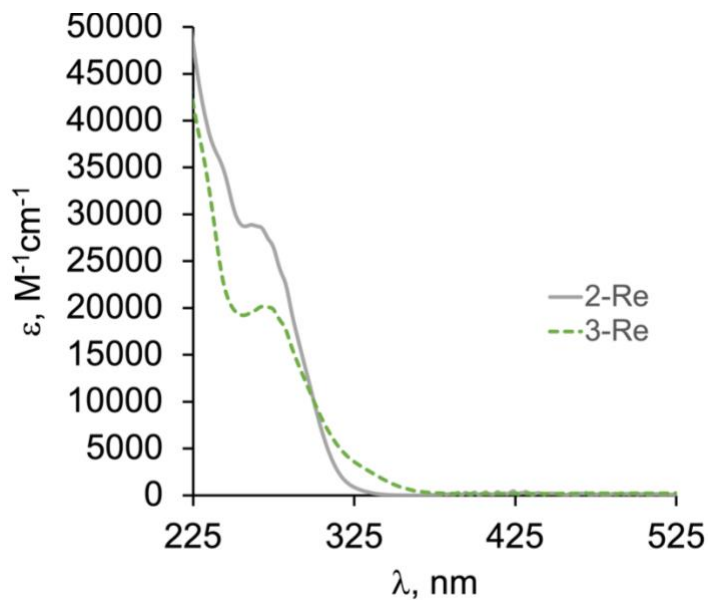


Figure S14. Overlay of electronic absorption spectra of **2-Re** and **3-Re** in CH_3CN .

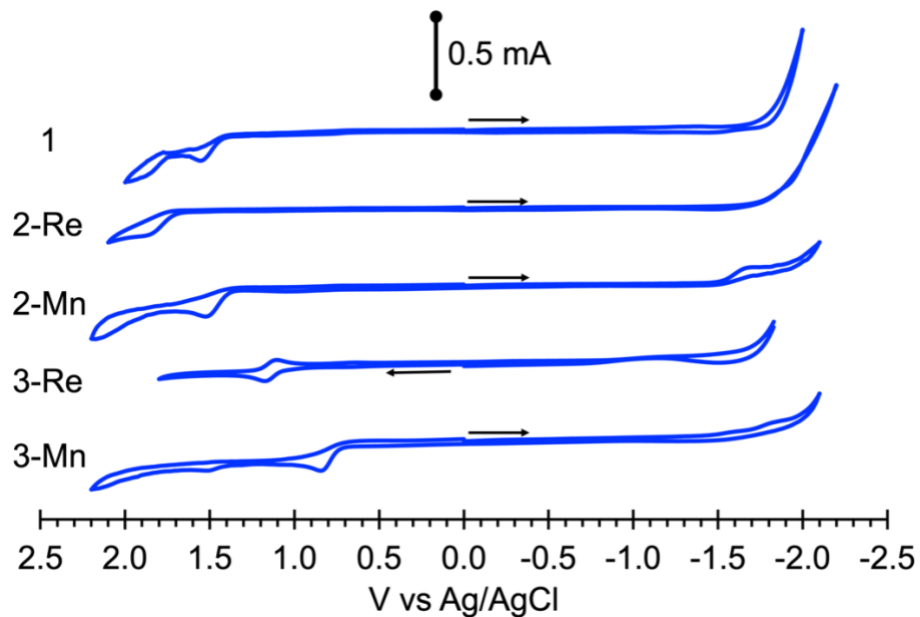


Figure S15. Cyclic voltammograms (200 mV/S) of new compounds ($\sim 1 \text{ mM}$ in CH_3CN) with NBu_4PF_6 as supporting electrolyte.

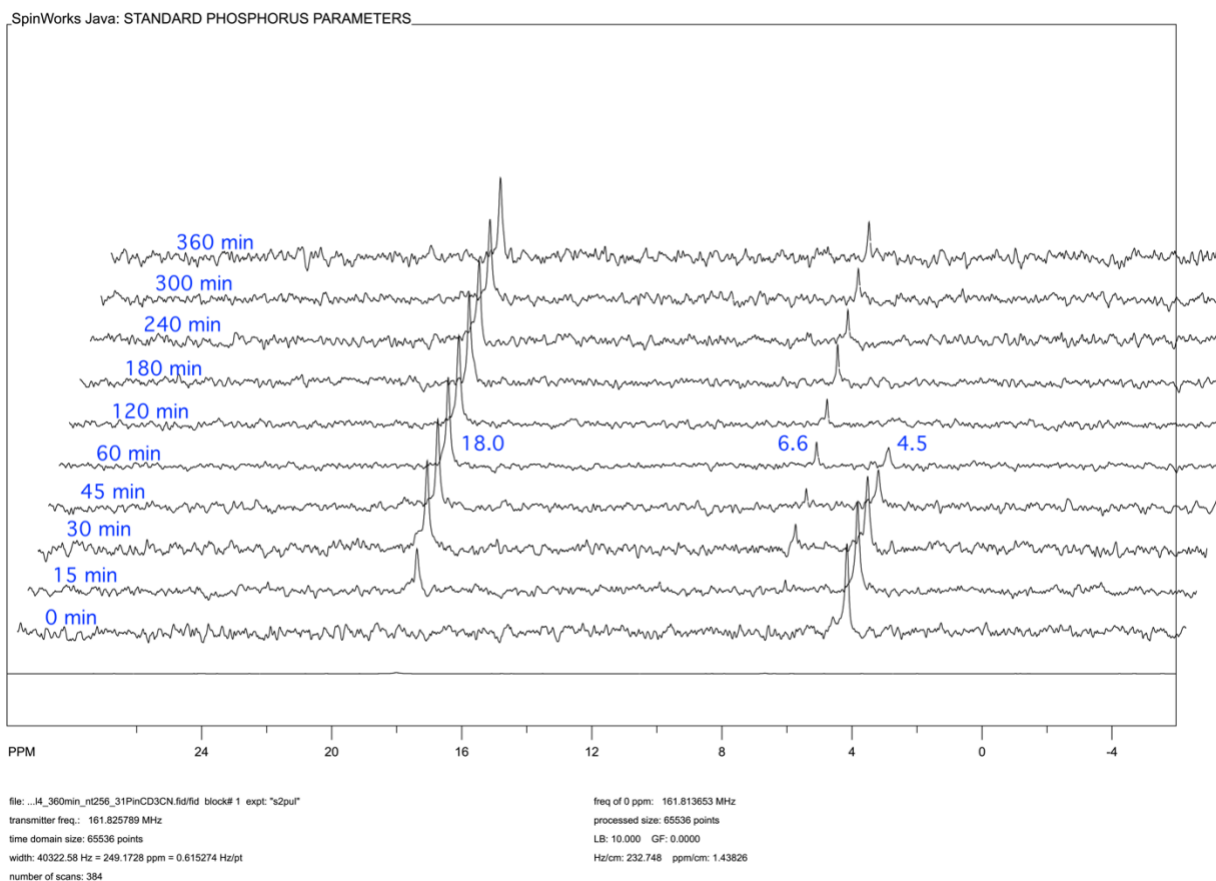


Figure S16. Overlay of ^{31}P NMR spectra obtained during photoirradiation of a CD_3CN solution of **2-Re** by UV-C light.

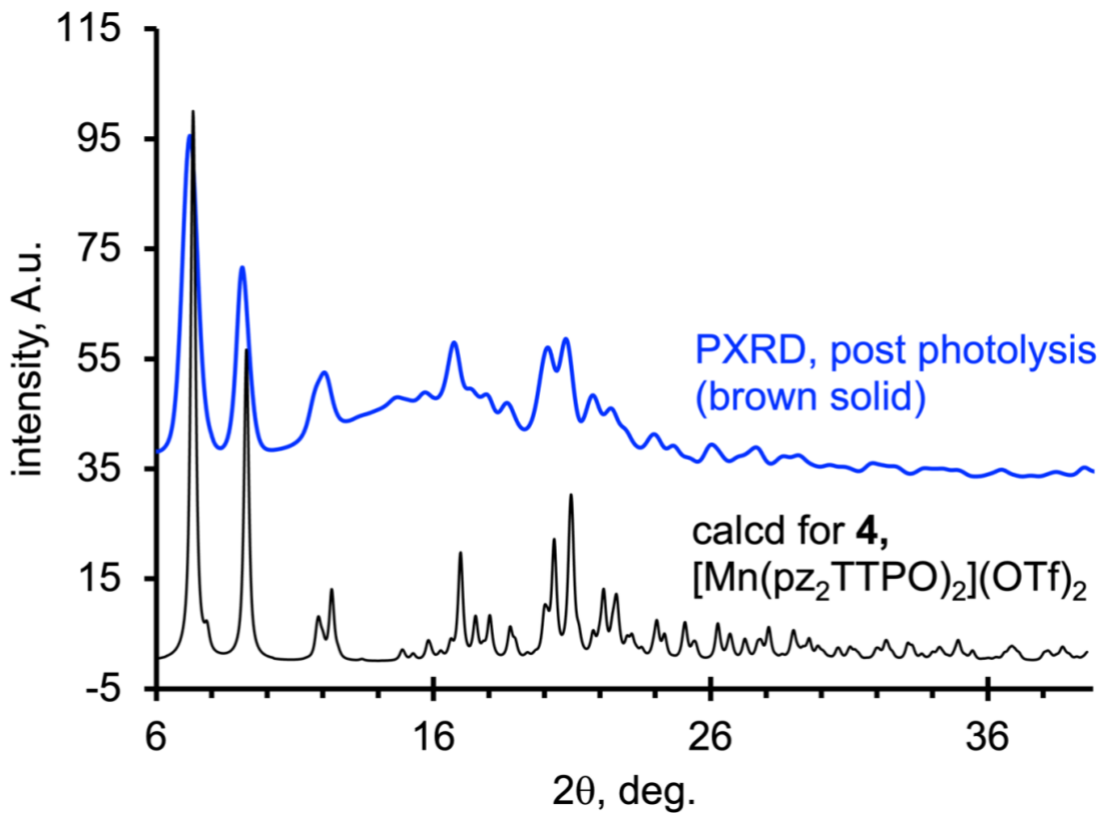


Figure S17. Diffractogram of crude brown product obtained after removing solvent from photodecomposition of **2-Mn** by 390 nm light (top blue trace), showing a mixture of an amorphous phase and **4**. Diffractogram of **4** (bottom black trace) calculated from single crystal diffraction data.

Table S3. Summary of SCF energies and Thermodynamic Properties for various compounds at the M06L/Def2TZVP (PCM CH₃CN) level.

Compound	S	E _{SCF} (a.u.)	ZPE corr (a.u.)	G (a.u.)	H (a.u.)	S (cal/mol*K)
CH ₃ CN	0	-132.796849765	0.045450	-132.775359	-132.746897	59.904
CO	0	-113.344569170	0.005011	-113.358678	-113.336253	47.198
[(pz ₂ TTP')Mn(CO) ₃] ⁰	^{1/2}	-3017.04415772	0.431237	-3016.680681	-3016.579103	213.789
[(pz ₂ TTP')Mn(CO) ₃] ⁺	0	-3016.95676838	0.435772	-3016.584959	-3016.488326	203.382
[(pz ₂ TTP')Mn(CO) ₃] ²⁺	^{1/2}	-3016.73548885	0.434785	-3016.365806	-3016.267326	207.267
	^{5/2}	-3016.71728756	0.428712	-3016.361905	-3016.251547	232.270
[(pz ₂ TTP')Mn(CO) ₂ (CH ₃ CN)] ⁰	^{1/2}	-3036.47075178	0.469408	-3036.069427	-3035.965805	218.089
[(pz ₂ TTP')Mn(CO) ₂ (CH ₃ CN)] ⁺	0	-3036.39036828	0.474213	-3035.982910	-3035.881795	212.816
[(pz ₂ TTP')Mn(CO) ₂ (CH ₃ CN)] ²⁺	^{1/2}	-3036.19727530	0.474286	-3035.791980	-3035.687405	220.098
	^{5/2}	-3036.19017508	0.468858	-3035.798104	-3035.682486	243.338
[(pz ₂ TTP')Mn(CO)(CH ₃ CN) ₂] ⁰	^{1/2}	-3055.88748577	0.507422	-3055.449420	-3055.342950	224.084
[(pz ₂ TTP')Mn(CO)(CH ₃ CN) ₂] ⁺	0	-3055.81236238	0.512958	-3055.369692	-3055.261947	226.767
[(pz ₂ TTP')Mn(CO)(CH ₃ CN) ₂] ²⁺	^{1/2}	-3055.65371876	0.514496	-3055.209263	-3055.101818	226.137
	^{5/2}	-3055.65877509	0.508604	-3055.229525	-3055.109568	252.469
[(pz ₂ TTP')Mn(CH ₃ CN) ₃] ⁰	^{1/2}	-3075.29461533	0.545182	-3074.823127	-3074.709075	240.043
[(pz ₂ TTP')Mn(CH ₃ CN) ₃] ⁺	0	-3075.22527170	0.550567	-3074.746148	-3074.635669	232.524
[(pz ₂ TTP')Mn(CH ₃ CN) ₃] ²⁺	^{1/2}	-3075.08848891	0.553206	-3074.607865	-3074.495692	236.089
	^{5/2}	-3075.12608556	0.548992	-3074.658212	-3074.534857	259.622
fac-[(pz ₂ TTP')Re(CO) ₃ Br] ⁻¹ (HBr)	^{1/2}	-4518.72202031	0.432334	-4518.361125	-4518.253621	226.261
fac-[(pz ₂ TTP')Re(CO) ₃ Br] ⁰ (HBr)	0	-4518.63791007	0.434419	-4518.273378	-4518.167809	222.188
fac-[(pz ₂ TTP')Re(CO) ₃ Br] ⁺¹ (HBr)	^{1/2}	-4518.42449136	0.433886	-4518.060966	-4517.954638	223.787
fac-[(pz ₂ TTP')Re(CO) ₃ Br] ⁰ (HCO)	0	-4518.63721758	0.434070	-4518.273544	-4518.167381	223.438
mer, trans-[(pz ₂ TTP')Re(CO) ₃ Br] ⁰	0	-4518.62067018	0.433820	-4518.256960	-4518.150987	223.038
mer, cis-[(pz ₂ TTP')Re(CO) ₃ Br] ⁰	0	-4518.60224517	0.433284	-4518.239965	-4518.132890	225.359
[(pz ₂ TTP')Re(CO) ₃] ⁰	^{1/2}	-1944.47670902	0.430063	-1944.112241	-1944.013254	208.336
[(pz ₂ TTP')Re(CO) ₃] ⁺	0	-1944.38912605	0.434967	-1944.019760	-1943.921074	207.702
[(pz ₂ TTP')Re(CO) ₃] ²⁺	^{1/2}	-1944.15837789	0.434511	-1943.789685	-1943.690521	208.709
[(pz ₂ TTP')Re(CO) ₂ (CH ₃ CN)] ⁰	^{1/2}	-1963.89860715	0.468672	-1963.497947	-1963.394914	216.852
[(pz ₂ TTP')Re(CO) ₂ (CH ₃ CN)] ⁺	0	-1963.81672168	0.473712	-1963.412803	-1963.307490	221.650
[(pz ₂ TTP')Re(CO) ₂ (CH ₃ CN)] ²⁺	^{1/2}	-1963.61412314	0.473825	-1963.210058	-1963.104571	222.016

pz₂TTP' = ligand with tolyl methyls replaced by H's

Table S4. Calculated IR CO and/or CN ($> 2200 \text{ cm}^{-1}$) stretching energies and intensities (Int) of bands of organic compounds and manganese complexes.

Compound M06L	S	IR cm-1	int	IR cm-1	int	IR cm-1	int	$\bar{\nu}_{\text{CO}}$
Def2-TZVP								
CH ₃ CN		2343.41	57.33					
		2296.54						
CO		2199.75	97.40					
		2155.76						2156
$[(\text{pz}_2\text{TPP}')\text{Mn}(\text{CO})_3]^0$	$1/2$	1870.65	2589.76	1875.49	2099.26	1982.41	2341.36	1910
		1823.88		1828.60		1932.85		1862
$[(\text{pz}_2\text{TPP}')\text{Mn}(\text{CO})_3]^+$	0	1993.91	1637.22	2009.67	1505.35	2093.27	1503.81	2032
		1944.06		1959.43		2040.94		1981
$[(\text{pz}_2\text{TPP}')\text{Mn}(\text{CO})_3]^{2+}$	$1/2$	2068.02	1095.36	2126.40	1046.33	2183.22	1293.01	2126
		2016.32		2073.24		2128.64		2073
	$5/2$	2251.76	90.92	2256.57	167.77	2265.22	166.37	2258
		2195.47		2200.16		2208.59		2201
$[(\text{pz}_2\text{TPP}')\text{Mn}(\text{CO})_2(\text{CH}_3\text{CN})]^0$	$1/2$	1918.70	1746.49	1989.84	1685.53	2359.48	32.55	1954
		1870.74		1940.10		2300.49		1905
$[(\text{pz}_2\text{TPP}')\text{Mn}(\text{CO})_2(\text{CH}_3\text{CN})]^+$	0	1945.69	1847.24	2013.22	1565.04	2369.01	4.62	1979
		1897.05		1962.89		2309.78		1930
$[(\text{pz}_2\text{TPP}')\text{Mn}(\text{CO})_2(\text{CH}_3\text{CN})]^{2+}$	$1/2$	2039.72	1218.98	2119.95	1227.06	2379.21	206.29	2080
		1988.73		2066.95		2319.73		2028
	$5/2$	2228.26	100.45	2248.054	150.74	2370.37	276.08	2238
		2172.56		2191.85		2311.11		2182
$[(\text{pz}_2\text{TPP}')\text{Mn}(\text{CO})(\text{CH}_3\text{CN})_2]^0$	$1/2$	1889.15	1927.93	2316.21	229.43	2336.49	208.73	2103
		1841.92		2258.30		2278.08		2050
$[(\text{pz}_2\text{TPP}')\text{Mn}(\text{CO})(\text{CH}_3\text{CN})_2]^+$	0	1918.38	2060.30	2329.68	135.04	2351.24	77.25	1918
		1870.42		2271.44		2292.46		1870
$[(\text{pz}_2\text{TPP}')\text{Mn}(\text{CO})(\text{CH}_3\text{CN})]^{2+}$	$1/2$	2029.85	1511.49	2373.72	76.64	2382.80	111.50	2030
		1979.10		2314.38		2323.23		1979
	$5/2$	2227.74	135.31	2368.59	219.13	2371.67	221.39	2228
		2172.04		2309.37		2312.38		2172
$[(\text{pz}_2\text{TPP}')\text{Mn}(\text{CH}_3\text{CN})_3]^0$	$1/2$	2259.09	829.65	2274.97	575.94	2307.41	640.08	
		2202.62		2218.10		2249.72		
$[(\text{pz}_2\text{TPP}')\text{Mn}(\text{CH}_3\text{CN})_3]^+$	0	2278.29	638.42	2295.38	398.97	2328.11	325.63	
		2221.34		2237.99		2269.90		
$[(\text{pz}_2\text{TPP}')\text{Mn}(\text{CH}_3\text{CN})_3]^{2+}$	$1/2$	2357.25	10.74	2360.34	8.67	2370.09	4.52	
		2298.32		2301.33		2310.84		
	$5/2$	2360.96	174.80	2369.57	184.16	2372.97	196.28	
		2301.94		2310.33		2313.65		

pz₂TPP' = ligand with tolyl methyls replaced by H's

Bold values after and empirical correction factor for pure organic compounds: $\bar{\nu}_{\text{corr}} = 0.98 * \bar{\nu}_{\text{raw}}$

Empirical correction factor for metal complexes: $\bar{\nu}_{\text{corr}} = 0.975 * \bar{\nu}_{\text{raw}}$

Table S5. Calculated IR CO and/or CN ($> 2200 \text{ cm}^{-1}$) stretching energies and intensities (Int) of bands of rhenium complexes.

Compound M06L	S	IR cm^{-1}	int	IR cm^{-1}	int	IR cm^{-1}	int	$\bar{\nu}_{\text{CO}}$
Def2-TZVP								
<i>fac</i> -{(pz ₂ TTP')Re(CO) ₃ Br} ⁰ (HCO)	0	1940.27	2267.07	1966.95	2045.60	2073.38	1679.34	1994
		1891.76		1917.78		2021.55		1944
<i>fac</i> -{[(pz ₂ TTP')Re(CO) ₃ Br] ⁰ (HBr)}	0	1939.98	2293.97	1968.54	2016.05	2074.18	1740.99	1994
		1891.48		1919.33		2022.33		1944
<i>mer,trans</i> -{[(pz ₂ TTP')Re(CO) ₃ Br] ⁰ }	0	1957.96	2025.80	1975.79	3905.87	2098.60	188.19	2011
		1909.01		1926.40		2046.13		1961
<i>mer,cis</i> {[(pz ₂ TTP')Re(CO) ₃ Br] ⁰ }	0	1952.64	4175.32	1959.15	2064.27	2086.09	395.45	1999
		1903.83		1910.17		2033.94		1949
[(pz ₂ TTP')Re(CO) ₃] ⁰	1/2	1943.37	2041.71	1950.90	2341.37	2058.88	2627.43	1984
		1894.79		1902.13		2007.41		1935
[(pz ₂ TTP')Re(CO) ₃] ⁺	0	1965.05	2205.11	1978.42	2063.51	2083.50	1650.83	2009
		1915.92		1928.95		2031.41		1959
[(pz ₂ TTP')Re(CO) ₃] ²⁺	1/2	2044.51	1111.60	2056.84	1220.43	2112.18	2808.15	2071
		1993.40		2005.42		2059.38		2019
[(pz ₂ TTP')Re(CO) ₂ (CH ₃ CN)] ⁰	1/2	1883.54	2291.85	1964.84	2121.77	2348.39	62.25	1924
		1836.45		1915.71		2289.68		1876
[(pz ₂ TTP')Re(CO) ₂ (CH ₃ CN)] ⁺	0	1912.49	2453.70	1990.99	1907.45	2360.95	6.50	1952
		1864.68		1941.22		2421.49		1903
[(pz ₂ TTP')Re(CO) ₂ (CH ₃ CN)] ²⁺	1/2	1981.11	1743.47	2076.37	1734.10	2360.78	208.18	2029
		1931.58		2024.46		2301.76		1978

pz₂TTP' = ligand with tolyl methyls replaced by H's

Bold values are with an empirical correction factor for metal complexes: $\bar{\nu}_{\text{corr}} = 0.975 * \bar{\nu}_{\text{raw}}$

Calculated Redox potentials.

The thermodynamic data in Table S3 were used to estimate redox potentials that are found in Table 3 of the main text. Briefly, for the reduction of a species according to Equations S-1 and S-2, the electrochemical potential of the reaction is calculated from the difference in



$$E^0 = -\Delta G/nF \quad \text{Equation S-2}$$

free energies ($627.5295 \text{ kcal}\cdot\text{mol}^{-1}/\text{Hartree}$) of the solvated complexes divided by $-F$ (since $n = 1$ mol e^- , $F = -23.06125 \text{ kcal}\cdot\text{mol}^{-1}/\text{eV}$ or by converting ΔG (Hartree) to E (eV) via $\Delta G^* = -27.2114 \text{ eV/Hartree}$), minus the absolute potential of the solvated electron (assigned value of 4.44 V vs SHE).

Thus for **2-Reⁿ⁺**, the energy minimized structures of the dication, monocation, and charge neutral reduced species were calculated in CH₃CN (PCM). For rhenium, with a ReN₂P(CO)₃ core, low spin states are calculated (and found) to be lowest energy for each of the three species. So, the reduction potential of the **(2-Re)⁺/(2-Re)⁰** couple is calculated using values (from Table S3):

$$E^0 \text{ (rxn)} = [(G_{\text{prod}} - G_{\text{react}})/-F] - E^0(e^- \text{ solv})$$

$$(-1944.112241 - -1944.019760 \text{ hartree}) * -27.2114 \text{ eV/Hartree} = 2.516 \text{ eV}$$

$$2.516 - 4.44 \text{ eV} = -1.92 \text{ V vs NHE}$$

Similarly, the **(2-Re)²⁺/(2-Re)⁺** couple is:

$$[(-1944.019760 - -1943.789685 \text{ hartree}) * -27.2114 \text{ eV/Hartree}] - 4.44 \text{ eV} = +1.82 \text{ V vs NHE}$$

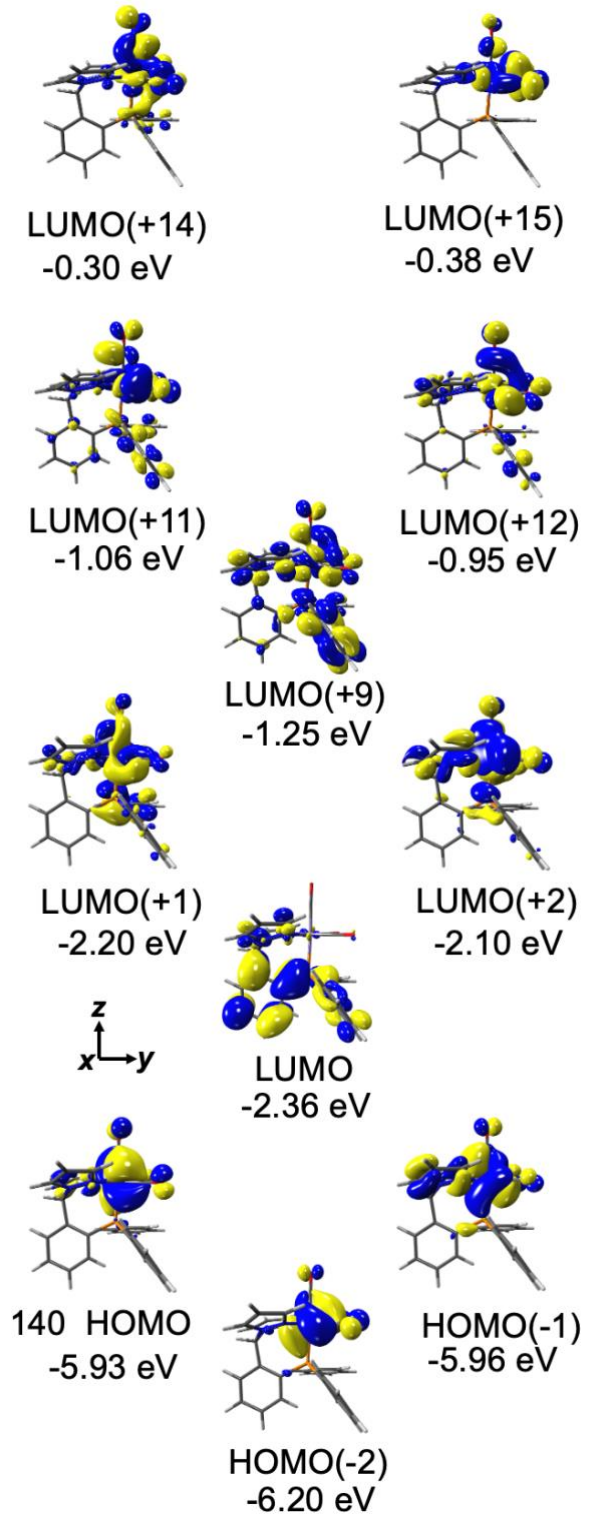


Figure S18. Frontier orbitals for **2-Mn**.

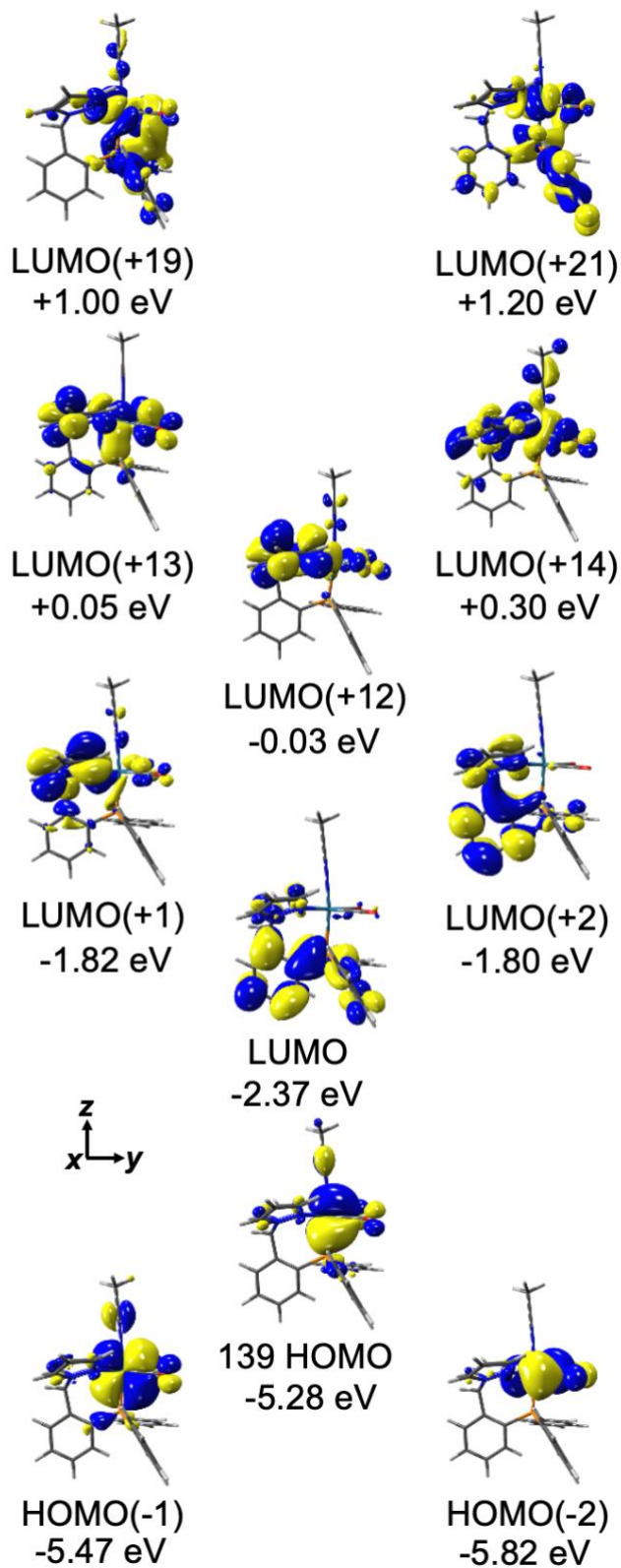


Figure S19. Frontier orbitals for **3-Re**.

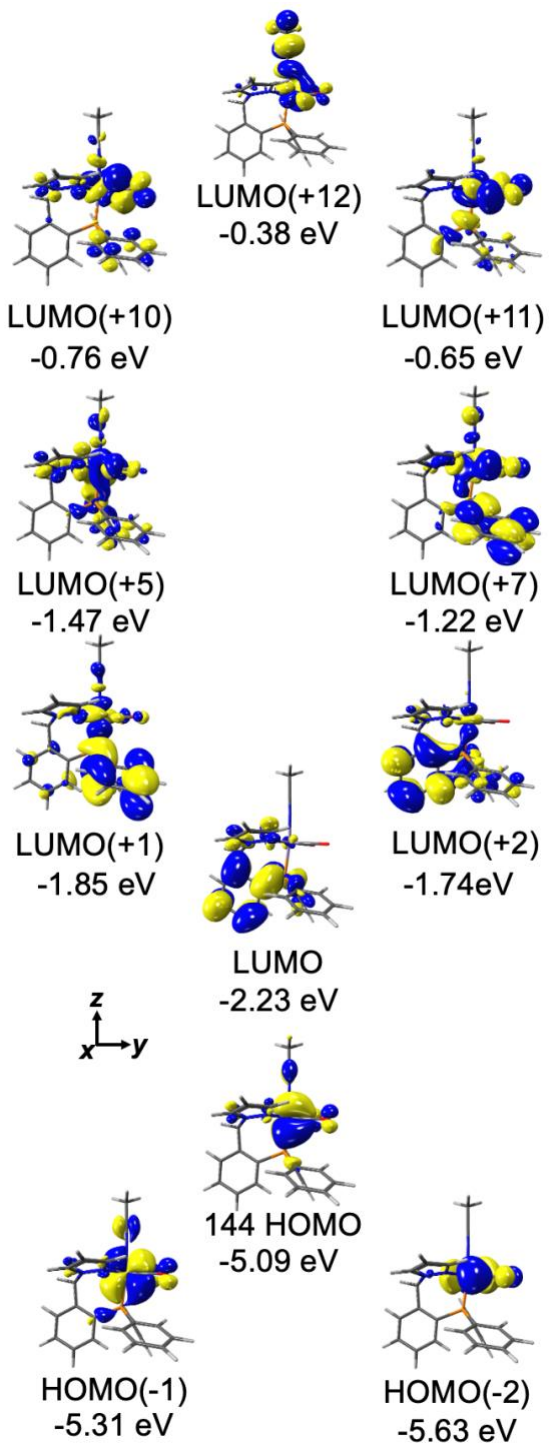


Figure S20. Frontier Orbitals for 3-Mn.

Table S6. Summary of TD-DFT (M06L/Def2-SV(P)/PCM CH₃CN) results for **1**,
 E(TD-HF/TD-DFT): -4516.35370235 hartree

state	eV	nm	f	<S2>	origin ^a	
1	3.5204	352.187251	0.0057	0	153->154	0.70462
2	3.6129	343.170306	0.0045	0	152->154	0.70010
3	3.7789	328.095478	0.0034	0	153->155	0.69118
4	3.8544	321.668742	0.0021	0	152->155	0.69121
5	3.9077	317.281265	0.0066	0	153->156 153->157	0.67194 0.63212,
6	3.9556	313.439175	0.0035	0	152->156 152->156	0.30290 0.54196,
7	4.0053	309.549846	0.0055	0	152->157	0.35226
8	4.0482	306.269453	0.004	0	152->157	0.60426
9	4.1016	302.282036	0.0208	0	151->154	0.68063
10	4.1592	298.095788	0.0021	0	153->158	0.69337
11	4.2253	293.432419	0.0018	0	153->159	0.69620
12	4.2783	289.797349	0.0119	0	152->158	0.62519
13	4.3112	287.585823	0.0026	0	152->159	0.63595
14	4.3148	287.345879	0.0031	0	150->154	0.56852
15	4.389	282.488038	0.0323	0	151->155 149->154	0.54598 0.56037,
16	4.4501	278.609469	0.0021	0	151->156 151->156	0.39986 0.51080,
17	4.4705	277.338105	0.0075	0	149->154 153->160	-0.32929 0.47679,
18	4.4992	275.56899	0.0139	0	151->157 153->161	0.31433 0.51379,
19	4.5068	275.104287	0.0044	0	153->160	-0.39830
20	4.5174	274.458759	0.0012	0	148->154 151->157	0.58210 0.43454,
21	4.5391	273.146659	0.0107	0	148->154 152->160	0.30107 0.54925,
22	4.5649	271.602883	0.0022	0	147->154 147->154	-0.39681 0.44896,
23	4.5725	271.151449	0.0078	0	152->160 152->161	0.38550 0.52762,
24	4.5926	269.964726	0.0048	0	153->162	-0.40452
25	4.6109	268.893275	0.0056	0	150->155	0.57919

(a) Only transitions with intensity > 0.3 are reported; HOMO = orbital 153

Table S7. Summary of TD-DFT (M06L/Def2-SV(P)/PCM CH₃CN) results for **2-Re**,

E(TD-HF/TD-DFT): -1942.4047 hartree

state	eV	nm	f	$\langle S^2 \rangle$	origin ^a	
1	3.8572	321.435238	0.0069	0	135->136	0.70219
2	3.8895	318.765908	0.0043	0	134->136	0.69971
3	4.1754	296.939215	0.002	0	133->136	0.67836
4	4.2021	295.052474	0.0157	0	135->137	0.61069
5	4.2425	292.242781	0.0065	0	132->136	0.67628
6	4.256	291.315789	0.015	0	134->137	0.65570
7	4.3059	287.939804	0.0115	0	135->138	0.63401
8	4.3918	282.307938	0.0656	0	134->138	0.53904
9	4.4187	280.589314	0.0139	0	135->139	0.56110
10	4.4267	280.082228	0.0055	0	134->139	0.62564
11	4.447	278.803688	0.0026	0	131->136 134->140	0.63720 0.46340,
12	4.5139	274.67157	0.0075	0	133->137 134->140	0.37283 0.40082,
13	4.5306	273.659118	0.0032	0	135->140 130->136	-0.38769 0.41703,
14	4.5356	273.357439	0.0348	0	133->137 130->136	0.30985 0.36488,
15	4.541	273.032372	0.002	0	133->137	-0.33254
16	4.5873	270.276633	0.0202	0	132->137 129->136	0.55414 0.46667,
17	4.5981	269.641809	0.0132	0	133->138	0.32605
18	4.6356	267.460523	0.0416	0	133->138	0.52400
19	4.6769	265.098676	0.0025	0	132->138	0.61197
20	4.7042	263.560223	0.0054	0	133->139	0.55580
21	4.7147	262.973254	0.0008	0	134->141	0.50418
22	4.7305	262.094916	0.0047	0	135->141	0.49890
23	4.7668	260.099018	0.0139	0	131->137	0.61905
24	4.7797	259.397033	0.0018	0	132->139	0.62224
25	4.8058	257.988264	0.0067	0	130->137	0.55380

(b) Only transitions with intensity > 0.3 are reported; HOMO = orbital 135

Table S8. Summary of TD-DFT (M06L/Def2-SV(P)/PCM CH₃CN) results for **2-Mn**,

E(TD-HF/TD-DFT): -3014.85311724

	eV ^a	nm	f	<S2>	Origin ^b
				140 ->142	0.45652,
				140 ->141	0.39582,
1	3.5143875	352.789782	0.0051	0 139 ->143	0.32301
				140 ->141	0.58025,
2	3.537495	350.485301	0.0021	0 140 ->142	-0.34453
3	3.55836	348.430176	0.003	0 139 ->141	0.70258
4	3.7195275	333.332661	0.0302	0 139 ->142	0.59550
				140 ->143	0.36882,
				140 ->142	-0.31518,
5	3.8025975	326.050811	0.0247	0 139 ->143	0.30143
6	3.80757	325.625005	0.0017	0 138 ->141	0.68265
7	3.84696	322.290848	0.018	0 140 ->143	0.49018
				138 ->142	0.43112,
8	3.93939	314.72893	0.0049	0 138 ->143	-0.35922
				140 ->144	0.43888,
				138 ->143	-0.37847,
9	4.0250925	308.027704	0.0083	0 138 ->142	-0.30572
				140 ->144	0.53866,
10	4.0484925	306.247325	0.0009	0 138 ->143	0.31569
11	4.127565	300.380491	0.0027	0 139 ->144	0.68117
				137 ->141	0.59976,
12	4.1227875	300.728573	0.0065	0 140 ->145	-0.32188
				140 ->145	0.58440,
13	4.127565	300.380491	0.0044	0 137 ->141	0.34986
14	4.1855775	296.217189	0.0075	0 139 ->145	0.62207
				140 ->146	0.51428,
15	4.2031275	294.980345	0.0037	0 139 ->146	0.35036
				139 ->146	0.46570,
16	4.237935	292.557578	0.0327	0 137 ->142	-0.37421
17	4.30872	287.751351	0.0071	0 137 ->143	0.58676
18	4.316715	287.218406	0.0008	0 138 ->144	0.65265
				137 ->142	0.44880,
19	4.3372875	285.856079	0.0331	0 140 ->146	-0.30633
20	4.35279	284.838	0.0086	0 140 ->147	0.53628
				136 ->141	0.56601,
21	4.3718025	283.599271	0.0033	0 135 ->141	-0.38029
22	4.406025	281.396497	0.0126	0 139 ->147	0.53400,
				140 ->148	0.43655,
23	4.41987	280.515038	0.0034	0 138 ->145	0.38962
24	4.4529225	278.432872	0.0078	0 135 ->141	0.43628
				140 ->148	0.35580, 1
				38 ->146	-0.32781,
25	4.4538975	278.37192	0.0155	0 138 ->145	-0.32036

(a) An empirical scaling factor of 0.975 has been applied.

(b) Only transitions with intensity > 0.3 are reported; HOMO = orbital 140;

Table S9. Summary of TD-DFT (M06L/Def2-SV(P)/PCM CH₃CN) results for **3-Re**,

E(TD-HF/TD-DFT):		-1961.8327 hartree				
	eV	nm	f	<S2>	origin	
1	3.1563	392.814371	0.0055	0	139->140	0.70495
2	3.344	370.76555	0.0045	0	138->140	0.70403
3	3.6327	341.29986	0.0163	0	139->142	0.61873
4	3.6545	339.263921	0.0244	0	139->141	0.60404
5	3.7196	333.326164	0.0045	0	137->140 138->142	0.69431 0.57468,
6	3.8167	324.846071	0.0131	0	139->143	-0.31433
7	3.8228	324.327718	0.0309	0	139->143 138->141	0.58825 0.53825,
8	3.8632	320.936012	0.0426	0	139->144	0.31559
9	3.9121	316.924414	0.0167	0	139->144	0.58783
10	3.982	311.361125	0.0054	0	138->143	0.69113
11	4.1116	301.546843	0.0345	0	138->144	0.65589
12	4.1352	299.825885	0.0067	0	139->145 137->141	0.69971 0.58575,
13	4.1861	296.180215	0.0026	0	139->146	0.39196
14	4.2018	295.07354	0.0006	0	137->142 139->146	0.68262 0.50898,
15	4.2712	290.279078	0.0494	0	137->141 138->145	-0.33619 0.54538,
16	4.3252	286.654952	0.0037	0	139->147 139->147 138->145	-0.34647 0.47493, 0.37753,
17	4.3438	285.427506	0.0159	0	136->140 136->140	0.30560 0.59897,
18	4.3461	285.276455	0.021	0	139->147	-0.30613
19	4.3783	283.178403	0.0105	0	137->143	0.63003
20	4.4215	280.411625	0.017	0	138->146	0.60995
21	4.4431	279.048412	0.026	0	139->148	0.61927
22	4.4652	277.667294	0.0148	0	137->144 135->140	0.62052 0.54885,
23	4.476	276.997319	0.0034	0	134->140	0.37811
24	4.4922	275.998397	0.0058	0	138->147	0.69202
25	4.576	270.944056	0.038	0	134->140	0.55492

(a) Only transitions with intensity > 0.3 are reported; HOMO = orbital 139

Table S10. Summary of TD-DFT (M06L/Def2-SV(P)/PCM CH₃CN) results for **3-Mn**,

E(TD-HF/TD-DFT):		-3034.28880432 hartree				
	eV ^a	nm	f	<\$2>	origin ^b	
1	2.80488	442.029606	0.0042	0	144 ->145	0.70548
2	3.04317	407.417266	0.0031	0	143 ->145	0.69380
3	3.07476	403.231472	0.0112	0	144 ->146	0.63050
4	3.2560125	380.784779	0.0127	0	144 ->147	0.67318
5	3.28692	377.204191	0.0056	0	143 ->146	0.59745
6	3.354975	369.552679	0.0001	0	142 ->145	0.70363
7	3.3864675	366.116019	0.0188	0	144 ->148	0.68948
8	3.4749975	356.788746	0.0142	0	144 ->149	0.60794
9	3.484845	355.78053	0.0007	0	143 ->147 144 ->150	0.52216 0.48781,
10	3.5508525	349.166855	0.012	0	143 ->147	0.35290
11	3.6387975	340.727947	0.0205	0	143 ->148	0.65807
12	3.708705	334.305371	0.0124	0	143 ->149	0.61704
13	3.7158225	333.665023	0.0055	0	144 ->151	0.59984
14	3.7538475	330.285127	0.0082	0	142 ->146 143 ->150	0.55257 0.45650,
15	3.810885	325.341751	0.006	0	144 ->152	-0.36227
16	3.8291175	323.792623	0.007	0	142 ->147 142 ->147	0.53366 0.36760,
17	3.8704575	320.334224	0.0083	0	144 ->152	0.33785
18	3.886155	319.040285	0.0047	0	144 ->153	0.60635
19	3.936855	314.931589	0.0149	0	142 ->148	0.59471
20	3.97215	312.133228	0.0081	0	143 ->151	0.59024
21	3.9917475	310.600808	0.0098	0	142 ->149 144 ->154	0.56839 0.46904,
22	4.035525	307.231401	0.0232	0	142 ->149	0.30210
23	4.05756	305.562949	0.014	0	142 ->150	0.46647
24	4.1138175	301.384298	0.005	0	143 ->152	0.48830
25	4.14258	299.291746	0.019	0	143 ->153	0.63952

(a) An empirical scaling factor of 0.975 has been applied.

(b) Only transitions with intensity > 0.3 are reported; HOMO = orbital 144;

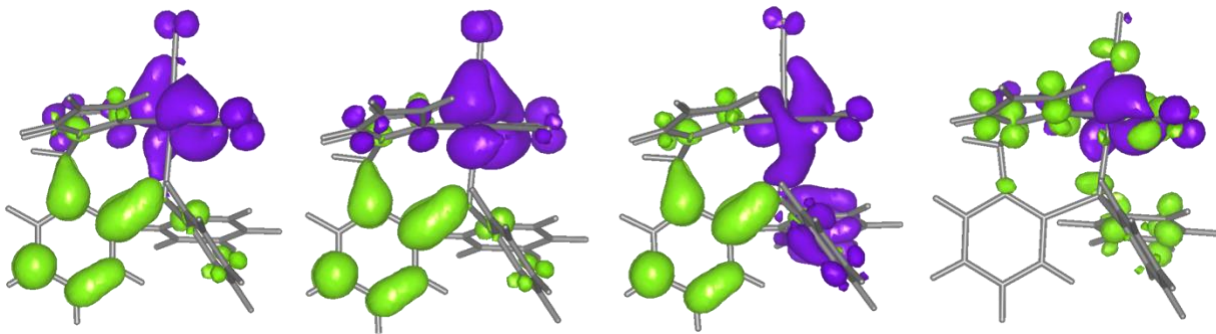


Figure S21. Electron density difference maps for first four excitations of **2-Re** using natural transition orbital analyses. Violet is negative (loss) while green is positive density (gain).

	1a	1b	2-Re	2-Mn	3-Re	3-Mn
M	0.58579	0.56587	0.5424	0.28062	0.66019	0.28317
Br	-0.6143	-0.6326				
P	0.43326	0.47792	0.47351	0.60423	0.48649	0.67178
N1					-0.5434	-0.5356
N12	-0.4565	-0.4385	-0.412	-0.2107	-0.4201	-0.2451
N22	-0.5951	-0.5918	-0.4166	-0.2376	-0.4217	-0.2217
C8	0.1797	0.17843	0.1835	0.07901	0.12208	-0.0105
O1	-0.3337	-0.3342	-0.3273	-0.2848	-0.3865	-0.34
C9	0.09903	0.09606	0.15919	0.04424	0.08486	0.032
O2	-0.3439	-0.3438	-0.3247	-0.2826	-0.3841	-0.3382
C10	0.19571	0.1764	0.19099	0.24128		
O3	-0.3045	-0.3072	-0.304	-0.2759		

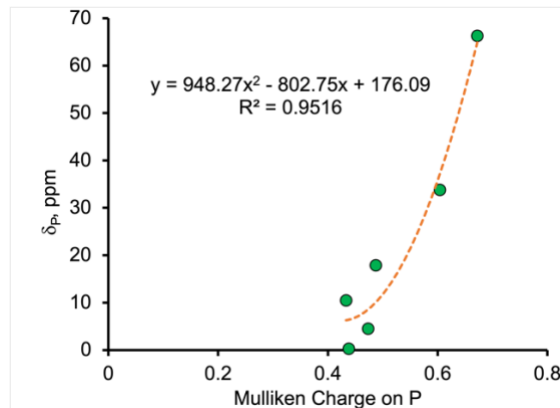


Figure S22. Left: Mulliken Charges on select atoms of **1a** (major isomer), **1b** (minor isomer), **2-M** and **3-M** (M = Re, Mn). Right: Plot of ^{31}P chemical shift versus phosphorous Mulliken charge.